

Final Report
UM-HSRI-80-75

Project No.
1150

ACCIDENT DATA SIMULATION
PEDESTRIAN AND SIDE IMPACT-3D

Prepared by:

D. H. Robbins
J. M. Becker
R. O. Bennett
B. M. Bowman
Highway Safety Research Institute
The University of Michigan
Ann Arbor, Michigan 48109

Prepared for:

Motor Vehicle Manufacturers Association, Inc.
320 New Center Building
Detroit, Michigan 48202

Date:

December 19, 1980



THE UNIVERSITY OF MICHIGAN
HIGHWAY SAFETY RESEARCH INSTITUTE

Final Report
UM-HSRI-80-75

Project No.
1150

ACCIDENT DATA SIMULATION
PEDESTRIAN AND SIDE IMPACT-3D

Prepared by:

D. H. Robbins
J. M. Becker
R. O. Bennett
B. M. Bowman
Highway Safety Research Institute
The University of Michigan
Ann Arbor, Michigan 48109

Prepared for:

Motor Vehicle Manufacturers Association, Inc.
320 New Center Building
Detroit, Michigan 48202

Date:

December 19, 1980

Technical Report Documentation Page

1. Report No. UM-HSRI-80-75		2. Government Accession No.		3. Recipient's Catalog No.	
4. Title and Subtitle Accident Data Simulation Pedestrian and Side Impact-3D				5. Report Date December 19, 1980	
				6. Performing Organization Code	
7. Author(s) Robbins, D.H., Becker, J.M., Bennett, R.O., and Bowman, B.M.				8. Performing Organization Report No. UM-HSRI-80-75	
				10. Work Unit No. 361727	
9. Performing Organization Name and Address Highway Safety Research Institute The University of Michigan Ann Arbor, Michigan 48109				11. Contract or Grant No. 1150	
				13. Type of Report and Period Covered Final - July 1979 - June 1980	
12. Sponsoring Agency Name and Address Motor Vehicle Manufacturers Association, Inc. 320 New Center Building Detroit, Michigan 48202				14. Sponsoring Agency Code	
				15. Supplementary Notes	
16. Abstract <p>The objective of this study has been to provide practical baseline data sets to describe a vehicle occupant in side impacts and to describe a pedestrian in frontal impacts. A concurrent project at HSRI, sponsored by NHTSA, included addition of mutual deformation and other features to the Calspan Three Dimensional occupant dynamics model. The baseline data sets were prepared to work with this new software and to represent advanced production vehicle design geometry.</p> <p>This report describes the baseline vehicle geometry in Part 2. The occupant and pedestrian, along with their contact interactions with the vehicle, are described in Parts 3 and 4. The baseline data sets and a sampling of the resulting computer program output are given in Part 5. A summary of information about the HSRI version of the Calspan occupant dynamics program is given in Part 6.</p>					
17. Key Words Automotive Safety Design Crash Dynamics Occupant Dynamics, Pedestrian Protection Restraint System			18. Distribution Statement Unlimited		
19. Security Classif. (of this report) Unclassified		20. Security Classif. (of this page) Unclassified		21. No. of Pages 82	22. Price

CONTENTS

	<u>Page</u>
1.0 Introduction	1
2.0 The Vehicles	2
2.1 Baseline Interior for Side Impact	2
2.2 Baseline Exterior for Pedestrian Impact	5
3.0 The Occupant and Pedestrian Models	8
3.1 Occupant for Side Impact Simulation	8
3.2 Pedestrian for Impact Simulation	8
4.0 Contact Interactions with the Vehicle	16
4.1 Vehicle Interior Force-Deformation Characteristics	16
4.1.1 Intrusion of Vehicle Components During Side Impact	21
4.2 Vehicle Exterior Force-Deformation Characteristics	21
5.0 The Computer Exercises	24
5.1 Vehicle Decelerations and Motions	24
5.2 Side Impact Input Data	26
5.3 Pedestrian Impact Input Data	46
5.4 Representative Side Impact Output	64
5.5 Representative Pedestrian Impact Output	68
6.0 The HSRI Version of the Calspan CVS	77
6.1 Modifications to Original Calspan CVS Program	77
6.2 Status of Software	81
7.0 References	82

LIST OF FIGURES

	<u>Page</u>
1. Vehicle Interior for Side Impact (Front View)	3
2. Vehicle Interior for Side Impact (Side View)	4
3. Vehicle Exterior for Pedestrian Impact (Side View)	6
4. Vehicle Exterior for Pedestrian Impact (Front View)	7
5. Occupant for Side Impact Simulation (Side View)	9
6. Occupant for Side Impact Simulation (Rear View)	10
7. Side View of Pedestrian (Initial Position)	12
8. Back View of Pedestrian (Initial Position)	13
9. Schematic of Euler Knee Joint	15
10. Panel Force-Deflection Curve	19
11. Side Window Force-Deflection Curve	20
12. Intrusion of Hip Panel Contact Surface	22
13. Side Impact Vehicle Acceleration Curve	25
14. Body Segment Accelerations. Side Impact	65
15. Body Segment Motions. Side Impact	66
16. Pedestrian Kinematics	70-72
17. Right Upper Shin Accelerations. Pedestrian Impact.	74
18. Right Lower Shin Accelerations. Pedestrian Impact.	74
19. Right Upper Leg Accelerations. Pedestrian Impact.	75
20. Lower Torso Accelerations. Pedestrian Impact.	75
21. Upper Torso Accelerations. Pedestrian Impact.	76
22. Head Accelerations. Pedestrian Impact.	76
23. Bivariate Force-Deflection -- Deflection Rate Input.	78
24. Corner Forces in British Leyland and MVMA 2-D Software	80

LIST OF TABLES

	<u>Page</u>
1. Occupant/Vehicle Interior Contacts	17
2. Pedestrian/Vehicle Exterior Contacts	18
3. Contents of Output of Input Table. Side Impact	27
4. Output of Baseline Input Data Set. Side Impact.	28
5. Listing of Baseline Side Impact Input Data File	40
6. Contents of Output of Input Table. Pedestrian Impact.	46
7. Output of Baseline Input Data Set. Pedestrian Impact.	47
8. Listing of Baseline Pedestrian Impact Input Data File	57
9. Changes to Baseline Pedestrian for Euler Joint Knee	63
10. Side Impact Occupant/Vehicle Contact History	67
11. Pedestrian/Vehicle Contact History	73
12. CVS Code Changes	81

1.0 INTRODUCTION

The objective of this study has been to provide practical baseline data sets to describe a vehicle occupant in side impacts and to describe a pedestrian in frontal impacts. During the past ten years a variety of projects have been conducted to study the interaction of pedestrians with motor vehicles. Somewhat more recently the emphasis has been on studying the interaction of a vehicle occupant with side door structures. Experimental studies have utilized both dummy and cadaver test subjects and a variety of vehicle types both experimental and production. Analytical studies have been conducted using both two- and three-dimensional dynamic occupant/pedestrian models.

A current project at HSRI, sponsored by NHTSA, includes addition of mutual deformation and other features to the Calspan Three Dimensional CVS model. The baseline data sets were prepared to work with this new software and to represent advanced production vehicle design geometry.

This report describes the baseline vehicle geometry in Part 2. The occupant and pedestrian along with their contact interactions with the vehicle are described in Parts 3 and 4. The baseline data sets and a sampling of the resulting computer program output are given in Part 5. A summary of information about the HSRI version of the Calspan CVS program is given in Part 6.

2.0 THE VEHICLES

In order to define the geometry of vehicle components with which an occupant might possibly interact during a side impact event or the front exterior components of a vehicle in the case of a pedestrian, it was necessary to obtain measurements from existing vehicles. Three vehicles were selected which are representative of the most modern domestic small car production.

For the front exterior of each vehicle, at least three points were measured with respect to a common inertial coordinate system to define the following surfaces approximately as planes:

- bumper
- grille
- hood
- windshield
- roof

For the vehicle interior the following surfaces were anticipated to be involved during lateral or 300° oblique impact:

- seat cushion
- seat back
- front door sill region (foot/lower leg contact)
- door panel lower region (hip and upper leg contact)
- door panel upper region (head contact)
- window panel (head contact)
- door header (head contact)
- floor (foot contact)
- B-pillar (head contact)

Other data were obtained which would make it possible to expand the simulation to cases of frontal impact.

2.1. BASELINE INTERIOR FOR SIDE IMPACT

Figures 1 and 2 illustrate the individual and average baseline panel locations which form the basis for construction of a side impact data set. These data are used in constructing the actual data sets described in Part 5 of this report.

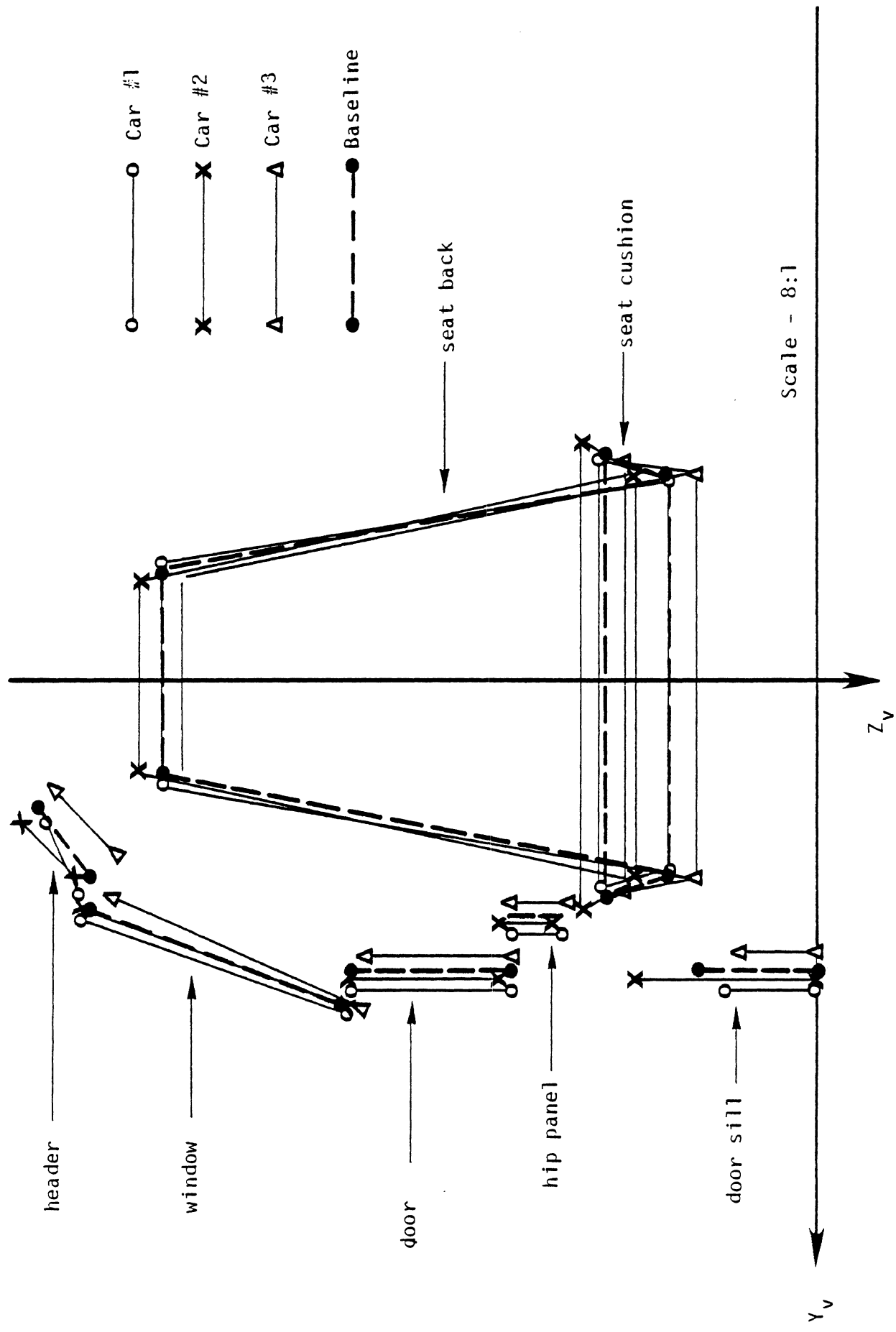


Figure 1. Vehicle interior for side impact (Front view)

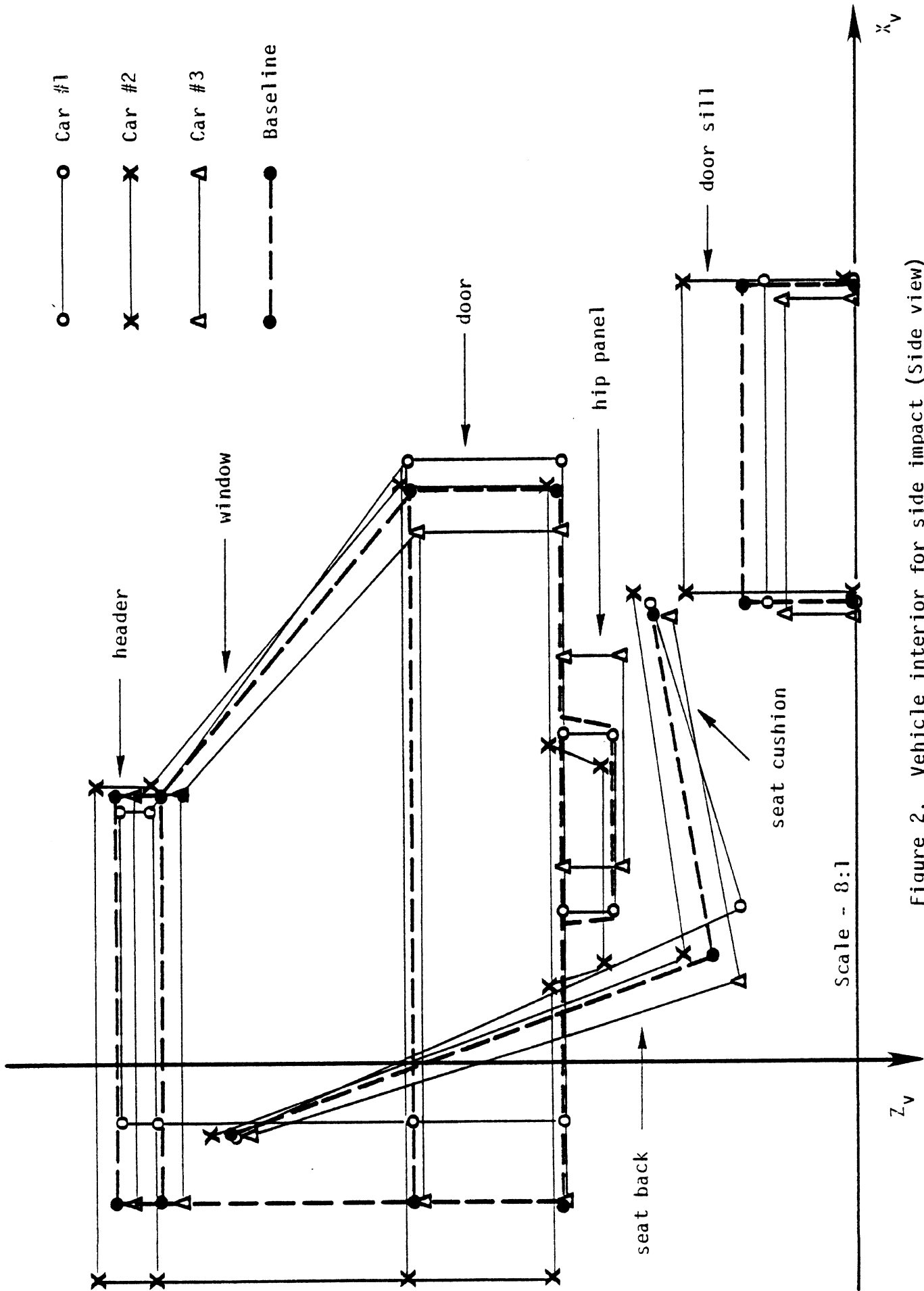


Figure 2. Vehicle interior for side impact (Side view)

2.2. BASELINE EXTERIOR FOR PEDESTRIAN IMPACT

Figures 3 and 4 illustrate the individual and average baseline panel locations which form the basis for a vehicle exterior intended for use in simulation of a pedestrian accident event. The baseline location has been used in constructing the actual data set described in Part 5 of this report. One surface which is not shown is the interface between the grille and hood. There was no clear definition for such a surface based on simple vehicle exterior measurements. Selection of a surface to represent this region was made to describe the stiff intersection between the grille and the hood.

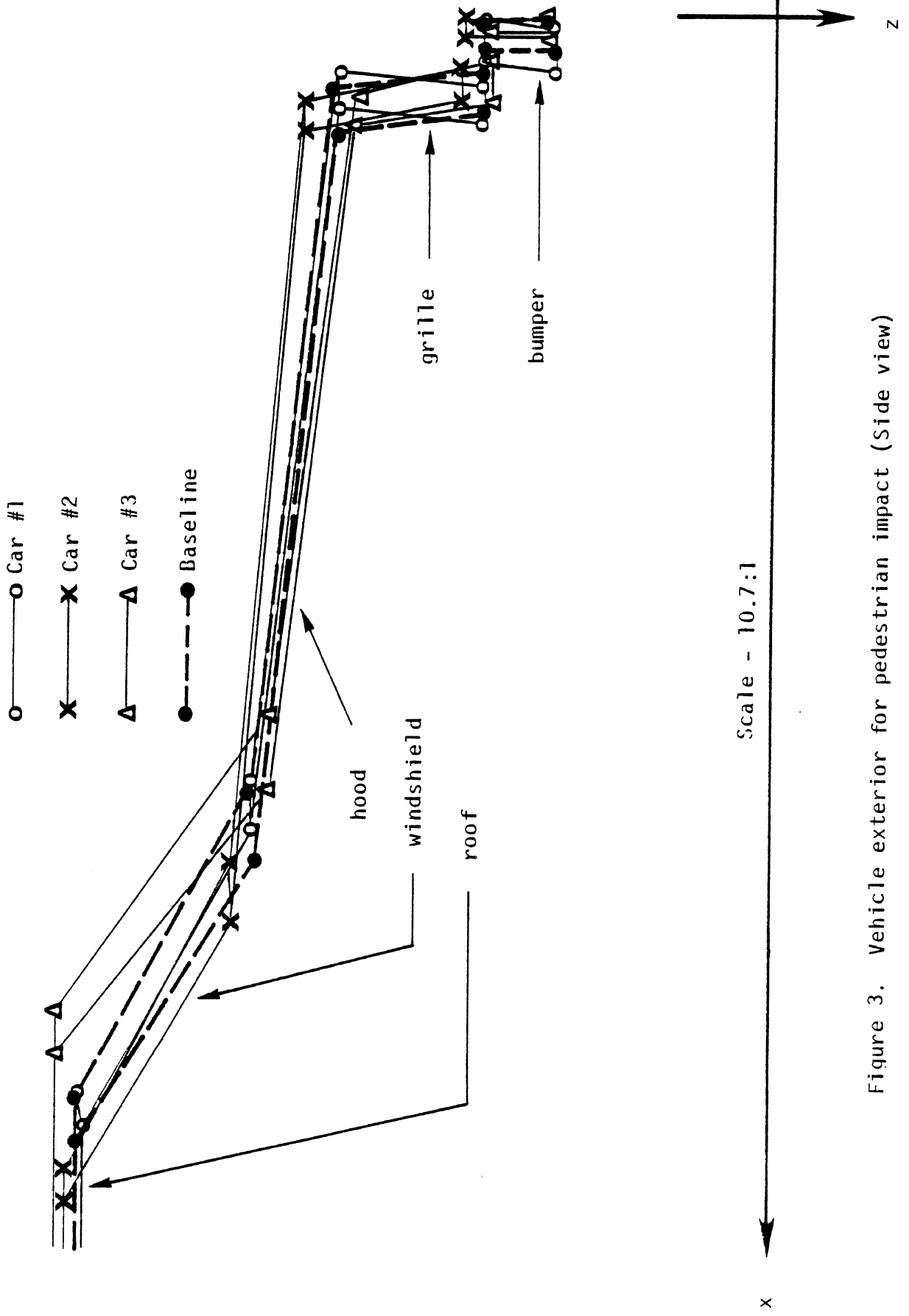


Figure 3. Vehicle exterior for pedestrian impact (Side view)

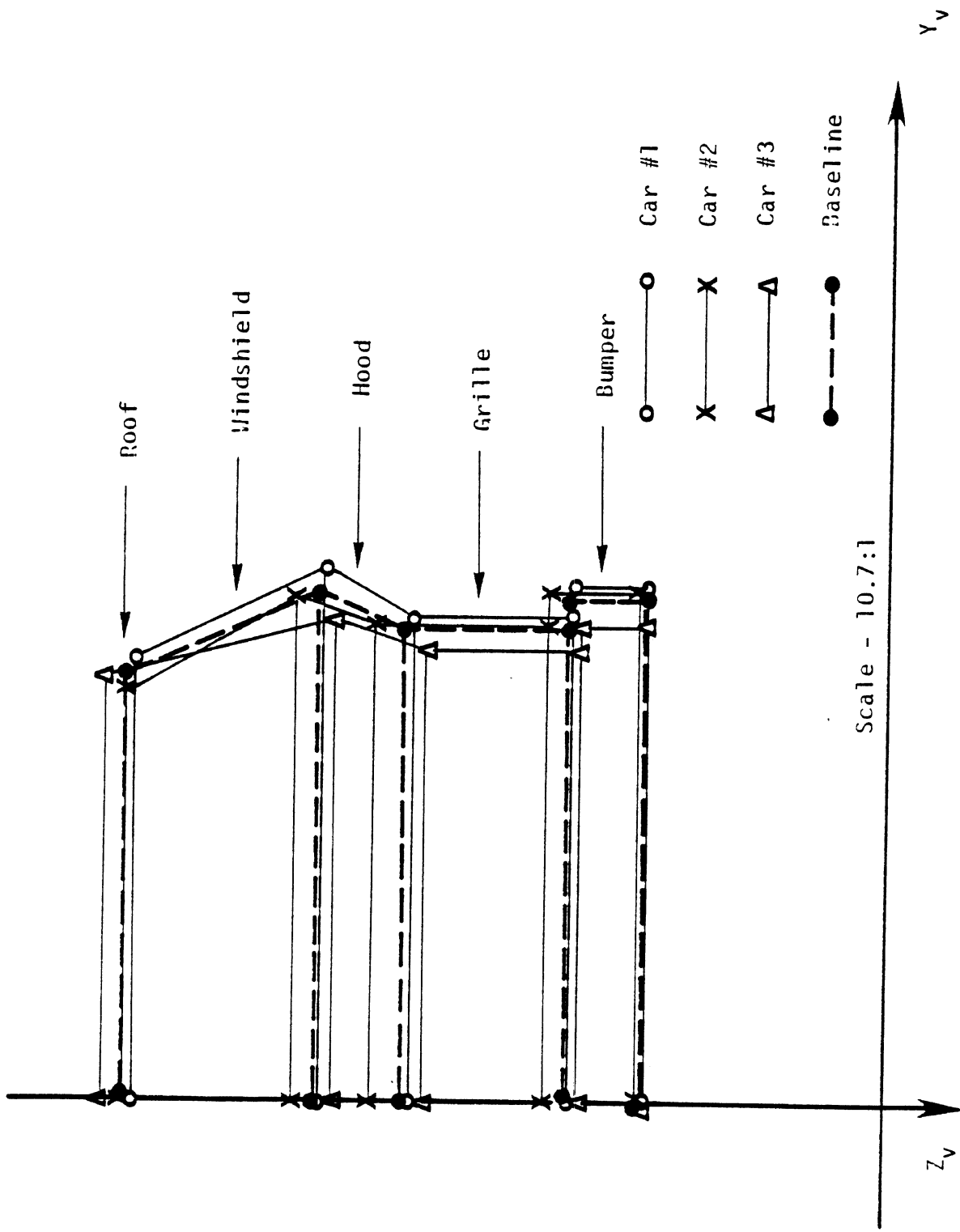


Figure 4. Vehicle exterior for pedestrian impact (Front view)

3.0 THE OCCUPANT AND PEDESTRIAN MODELS

A survey was conducted to identify sources for the most complete and recent data sets describing an occupant in a side impact simulation and a pedestrian. Surprisingly little information is publicly available beyond the original work done at Calspan (1).

With respect to the seated occupant, the primary data source was the sample data set provided with Calspan CVS Software, Version 18-A. This data set was used to verify model function in front impact before being modified slightly for the side impact case. The data on Part 572 developed for MVMA 2-D occupant modeling by Hubbard and McLeod (2) offered some promise but was restricted to two dimensions. Three-dimensional data, being developed at Calspan under an NHTSA contract, is not yet available.

For the pedestrian a Calspan data set modified by Karnes (3) was used as a starting point. These data were originally developed at General Motors and included a few changes from the standard seated occupant described in the preceding paragraph. Other than placing the subject in a standing position, hands were present and joint properties were changed. The reports from a major experimental and analytical study of pedestrian dynamics sponsored by NHTSA at Wayne State University were not yet available.

3.1 OCCUPANT FOR SIDE IMPACT SIMULATION

The occupant selected for the side impact simulation was essentially the same as that supplied with the sample data set included with Calspan CVS, Version 18-A. To position the occupant in the baseline seat required some minor vertical and horizontal adjustments in order to assure equilibrium. Figure 5 shows a side view of the occupant while Figure 6 shows a rear view. The numerical values for quantities such as segment mass, moments of inertia, position in space, ellipsoid axes, link angles, and joint properties are included in Part 5 which contains the complete listing of the output of the input data set.

3.2 PEDESTRIAN FOR IMPACT SIMULATION

The two pedestrian data sets which were developed on this project were derived largely from the data set reported by Karnes (3) of

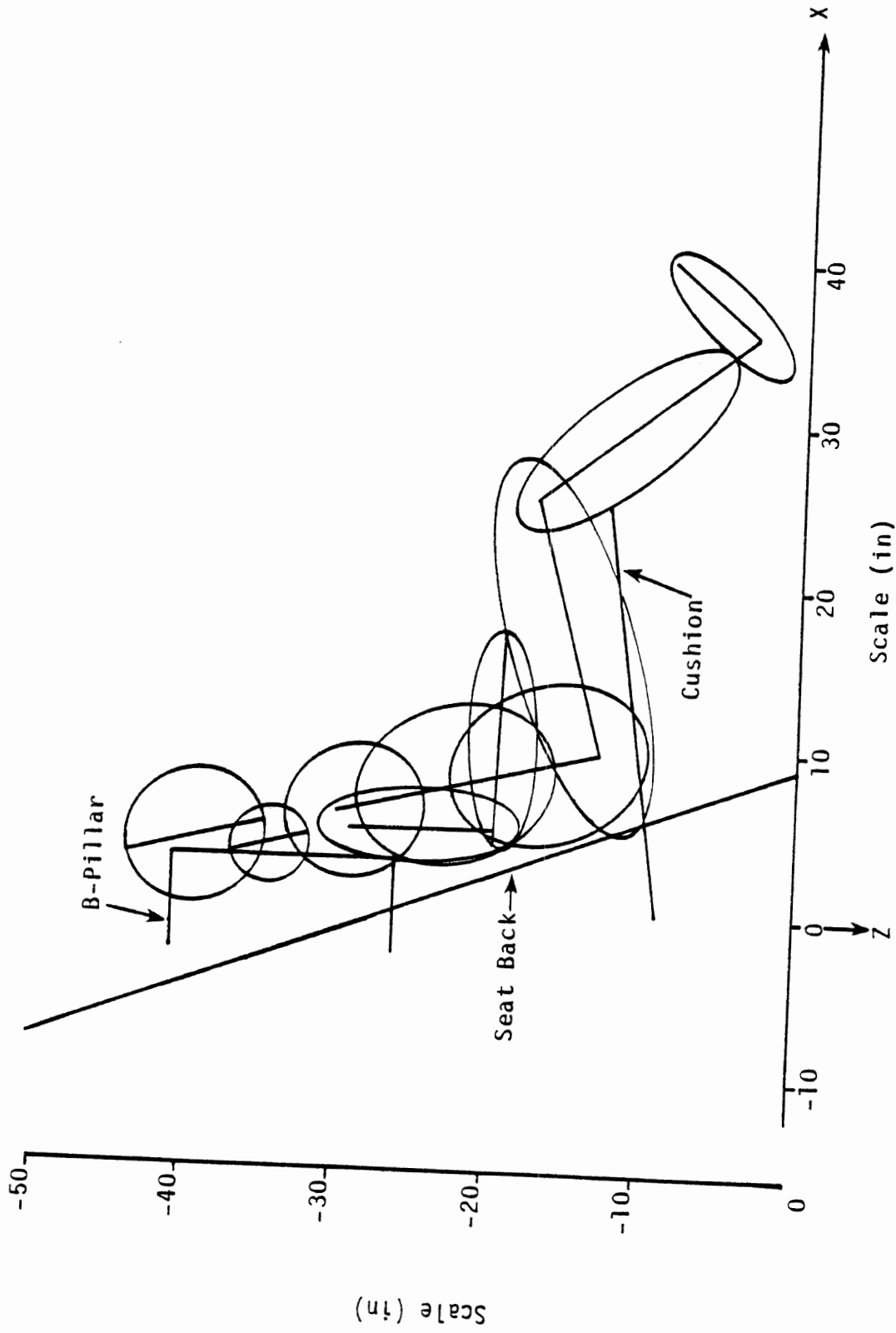


Fig. 5 Occupant for Side Impact Simulation (Side View)

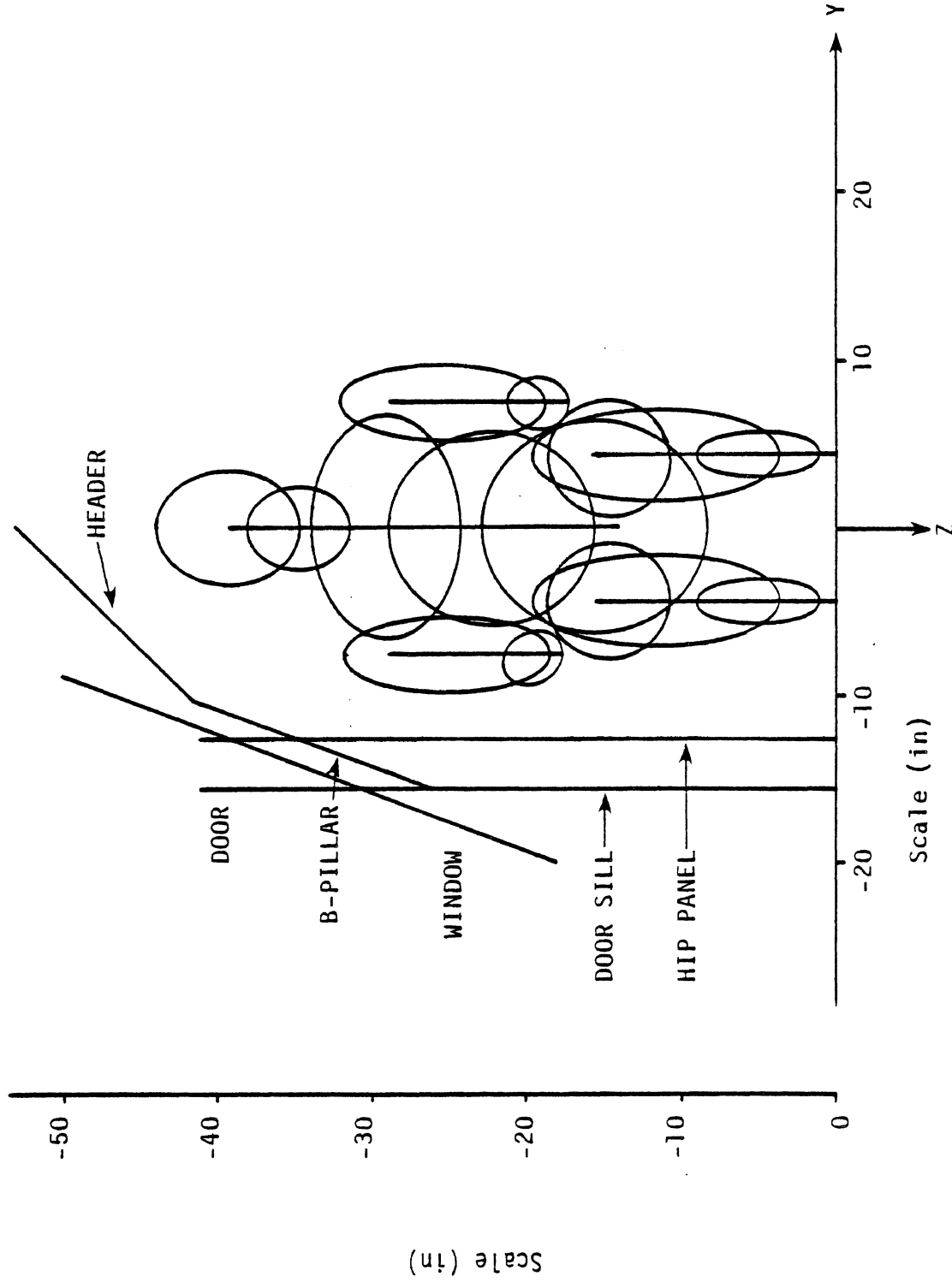


Fig. 6 Occupant for Side Impact Simulation (Rear View)

Boeing Computer Services. It describes the pedestrian as a modified Sierra 292-1050-2004 as has been used in the side impact case discussed in Section 3.1. The only difference is the addition of hands to the linkage. The masses and moments of inertia are identical, as are the joint locations, except for the hips and shoulders which are slightly different. The body ellipsoid semi-major axis lengths are similar but not identical. The joints are free of constraints. It is believed that this is due to the fact that a purpose of the simulation was to model the kinematics of a cadaver with no muscle tension to keep the body erect.

The major addition to the data set was the provision for fracturing of the lower leg and the knee. This was accomplished in two different ways, both of which included an extra joint within the shin (lower leg) mass.

The first case allowed a fracture to occur only in the shin. In order to do this the right lower leg has been partitioned into two segments by the addition of a new ball joint located 3.5 inches below the knee joint. This ball joint was initially locked with the capability of breaking free under a torque of 505.5 ft lb. This is based roughly on the work of Viano (4) and Kramer (5) who report femur and knee fracture loads of 4300 and 6000 N. If this load is applied at the center of a simply supported beam with a length of 18 inches, a torque of 505.5 ft lb is developed. This is used as a rough approximation of lower leg breaking load.

The masses and moments of inertia of the lower leg were then apportioned to the new upper and lower shin segments. A few minor modifications were made to some of the body ellipsoid axis lengths to eliminate unwanted interferences between body segment ellipsoids.

The initial standing posture of the pedestrian represents a person walking perpendicular to the path of the vehicle with 131.7 pounds of body weight supported by the right foot and 37.8 by the left. Figure 7 shows the left side of the pedestrian with the left front of the vehicle behind him. In Figure 8 the view is that of the back of the pedestrian with a front-to-rear section of the vehicle projected through

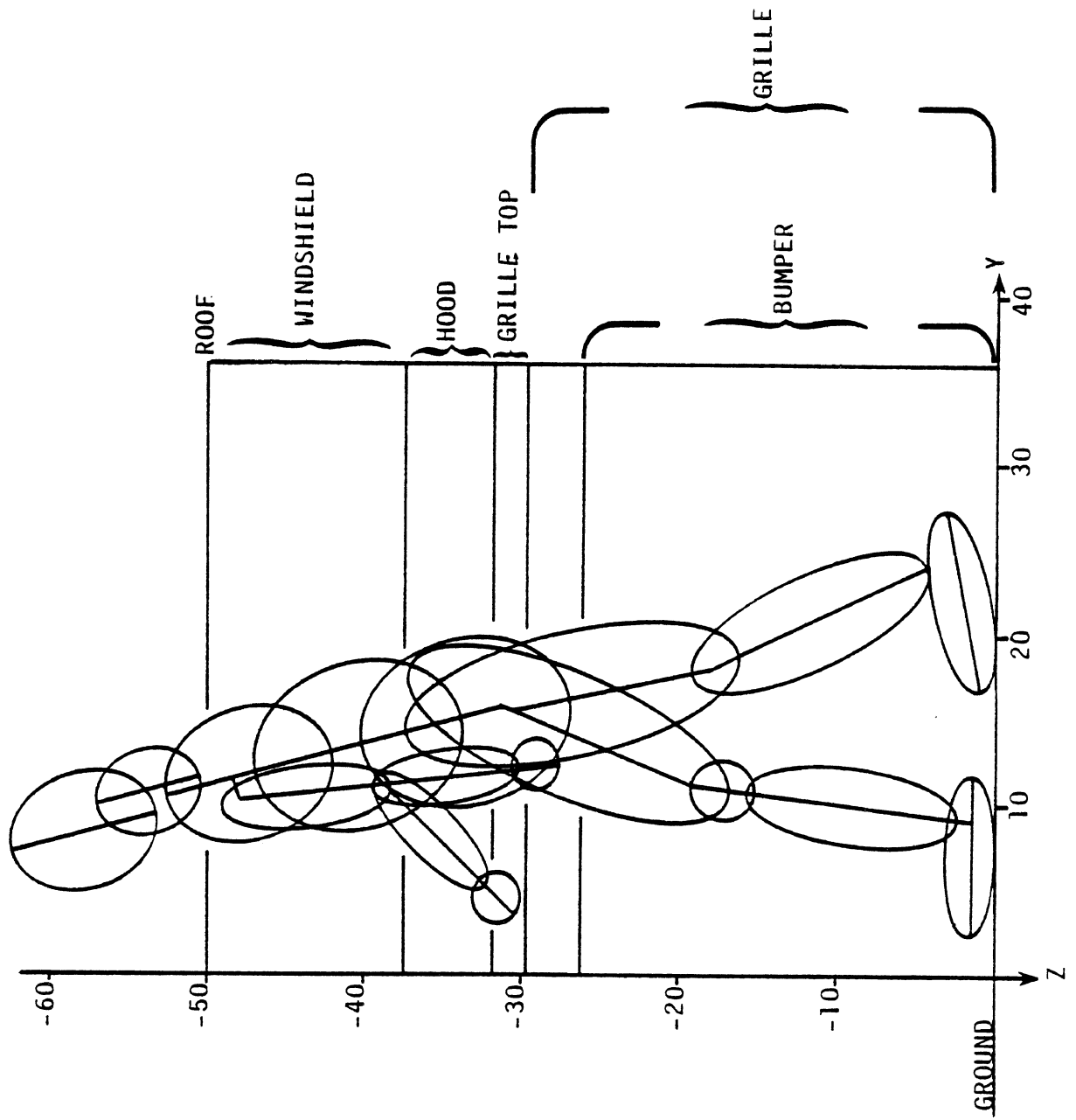


Fig. 7 Side View of Pedestrian (Initial Position).

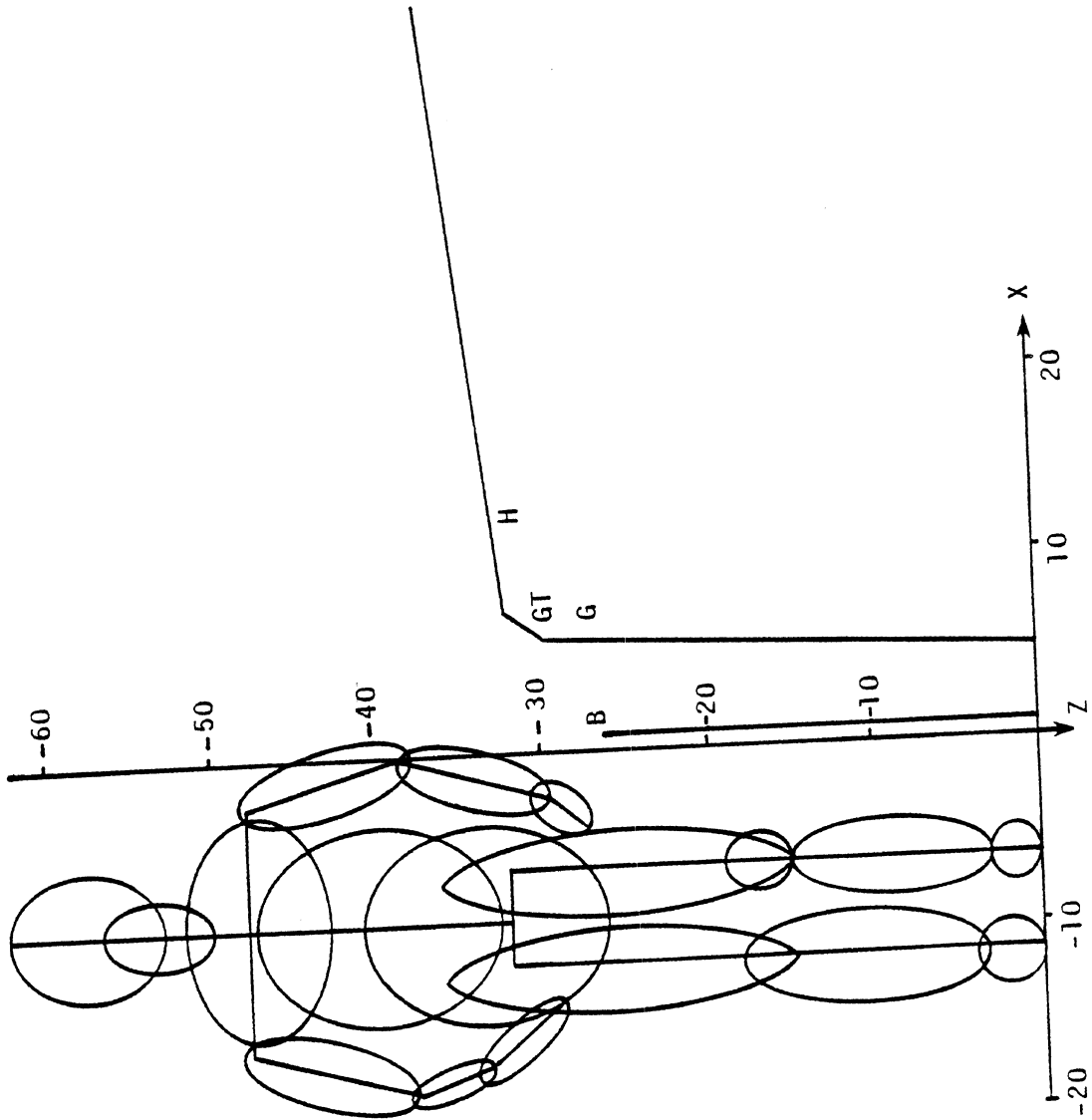


Fig. 8 Back View of Pedestrian (Initial Position)

the y-coordinate of the lower torso center of gravity. This section is on the left, or driver's, side of the vehicle.

The second case allows the fracture in the shin and also a fracture at the knee joint. This additional feature is accomplished by use of the Euler joint option (for which corrected code had been supplied by Calspan as a portion of CVS Version 19). Regular ball and socket joints have torques computed on the basis of two angles - flexure and torsion. The hinge joint uses only flexure. Figure 9 shows initial position of the pedestrian knee joint. This Euler joint has its torques computed on the basis of three angles - precession, nutation, and spin. Precession occurs about the Z-axis at the joint of the first segment. In this data set it is Z_u attached to the upper leg side of the joint. Spin occurs about the Z-axis at the joint of the second segment which in this case is Z_l attached to the upper shin side of the joint. Nutation occurs about an axis perpendicular to these two joint Z-axes. For the case of the knee joint shown in Figure 9, nutation corresponds to flexure and there is no locking of this degree of freedom. Precession and spin, however, are "unnatural" motions at this joint. Therefore, they are initially locked with a breakaway torque of 505.5 ft. lb. This value could be improved with data on lateral fractures or dislocations at the knee. A study should be conducted to compare results, cost of operation, and ease of data preparation for the several modeling options for locking "joints" and modeling fracture.

As in the case of the side impact simulation, the numerical value for quantities such as segment mass, moments of inertia, position in space, ellipsoid axes, link angles, and joint properties are included in Part 5 which contains the complete listing of the output of the input data set.

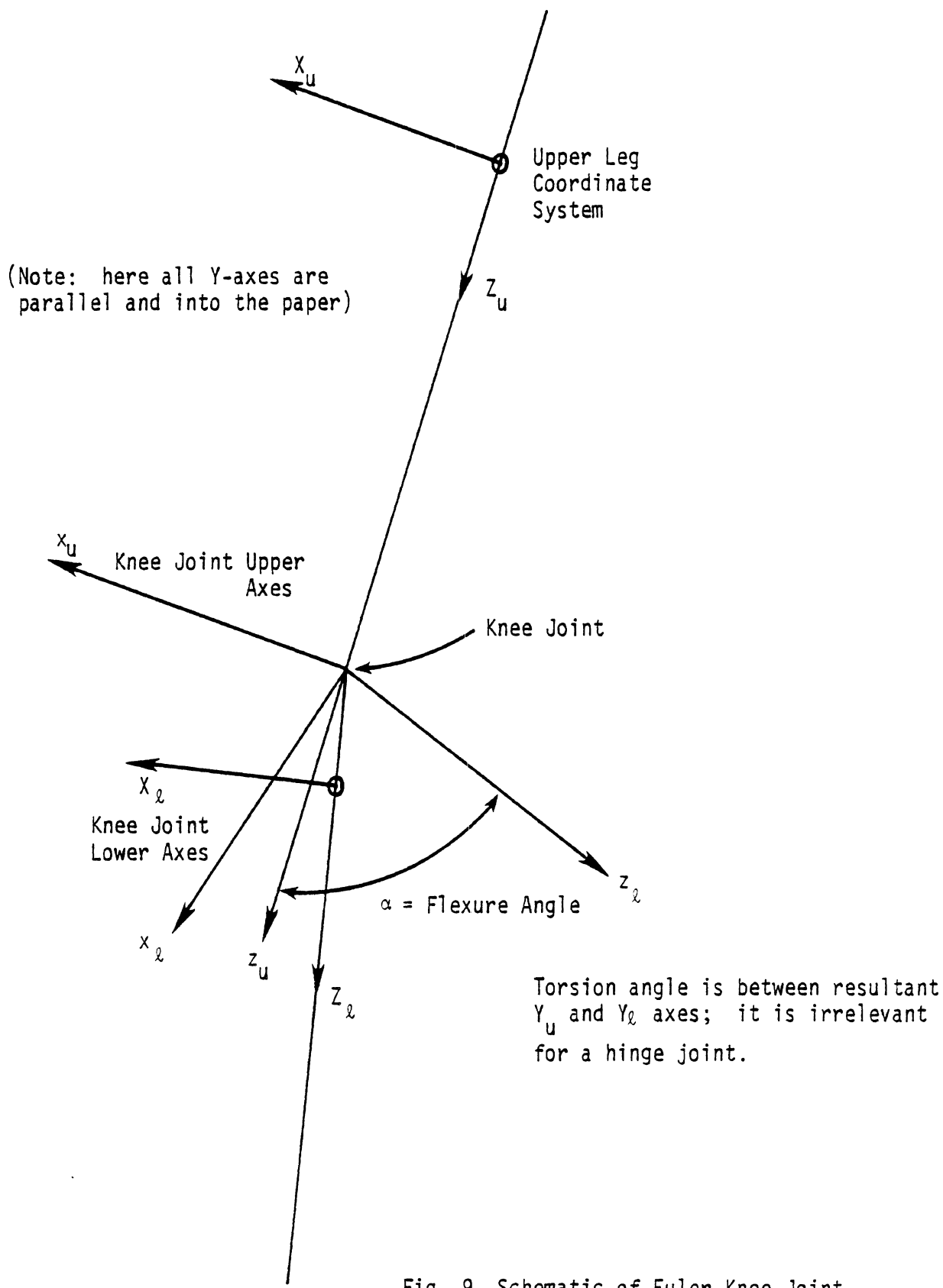


Fig. 9 Schematic of Euler Knee Joint

4.0 CONTACT INTERACTIONS WITH THE VEHICLE

A variety of contacts are allowed for both the occupant with the vehicle interior and the pedestrian with the vehicle exterior. Occupant or pedestrian ellipsoids may contact either flat panels attached to the vehicle or other of the ellipsoids on the subject. Table 1 shows the potential contacts which are allowed for the side impact occupant while Table 2 refers to the pedestrian.

The force-deflection characteristic curves governing interactions between the occupant or pedestrian and the vehicle have been derived from a variety of sources. Some are based on idealized vehicle component tests. Others are hypothetical estimates chosen to fill voids in our compilation of published, realistic vehicle descriptive data. All are intended to be treated as baseline data which should be replaced when measured data are available for use in actual engineering studies.

4.1 VEHICLE INTERIOR FORCE - DEFORMATION CHARACTERISTICS

Five different force-deflection characteristic curves are used to define the properties of the contact surfaces used to define the vehicle interior for side impact. Figure 10 illustrates the curve for a structure entitled, "panel." Tabular implementation of these data define the deformation of the header, front door sill, hip panel region, and B-pillar. The door panel shoulder region contact surface is modeled as a fifth order polynomial fit to the table. The symbol "x" on Figure 10 shows the closeness of fit of this polynomial. The polynomial form is used for this contact surface to allow mutual deformation of the vehicle and occupant thorax. These data are derived from dynamic deformation tests of door interiors and represent a somewhat stiffer structure than that used in recent side impact simulations by Padgaonkar and Prasad (6). Because of a lack of experimental information on the header, front door sill, and B-pillar, the data shown in Figure 10 have also been selected as hypothetical estimates for these surfaces.

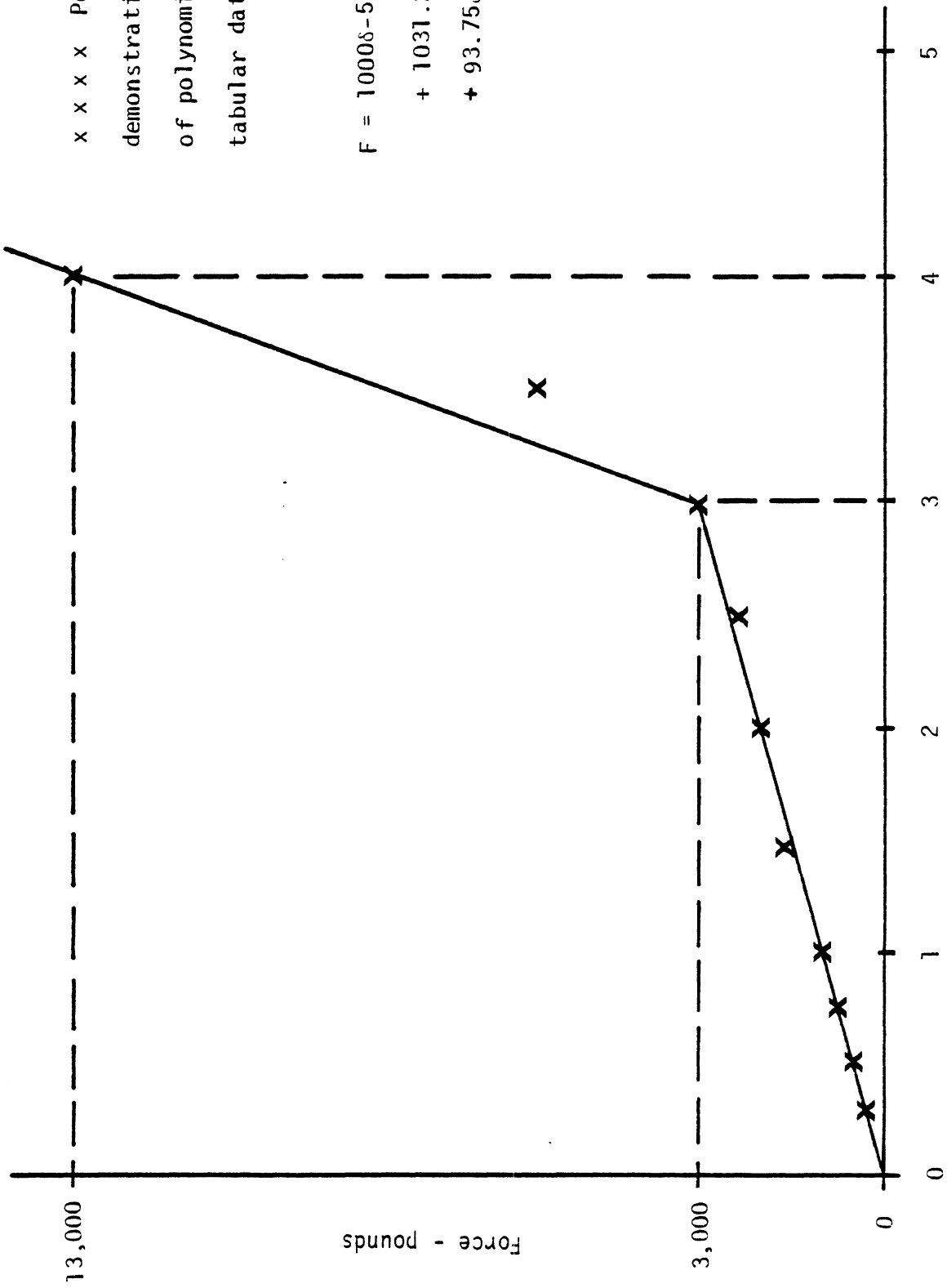
Figure 11 shows the representative force-deflection curve for side window tempered glass which has been selected for inclusion in the data.

TABLE 1. OCCUPANT/VEHICLE INTERIOR CONTACTS

<u>Ellipsoid Name</u>	<u>Contact Panel on Ellipsoid Name</u>
Lower torso	Seat back
Lower torso	Seat cushion
Lower torso	Hip panel
Lower torso	Right lower arm
Center torso	Seat back
Upper torso	Seat back
Upper torso	Door
Head	Header
Head	Window
Head	B-pillar
Right upper leg	Seat Cushion
Right upper leg	Left upper leg
Right lower leg	Left lower leg
Right foot	Floor
Right foot	Left foot
Left upper leg	Seat cushion
Left upper leg	Hip panel
Left lower leg	Door sill
Left foot	Floor
Left foot	Door sill
Left upper arm	B-pillar

TABLE 2. PEDESTRIAN/VEHICLE EXTERIOR CONTACTS

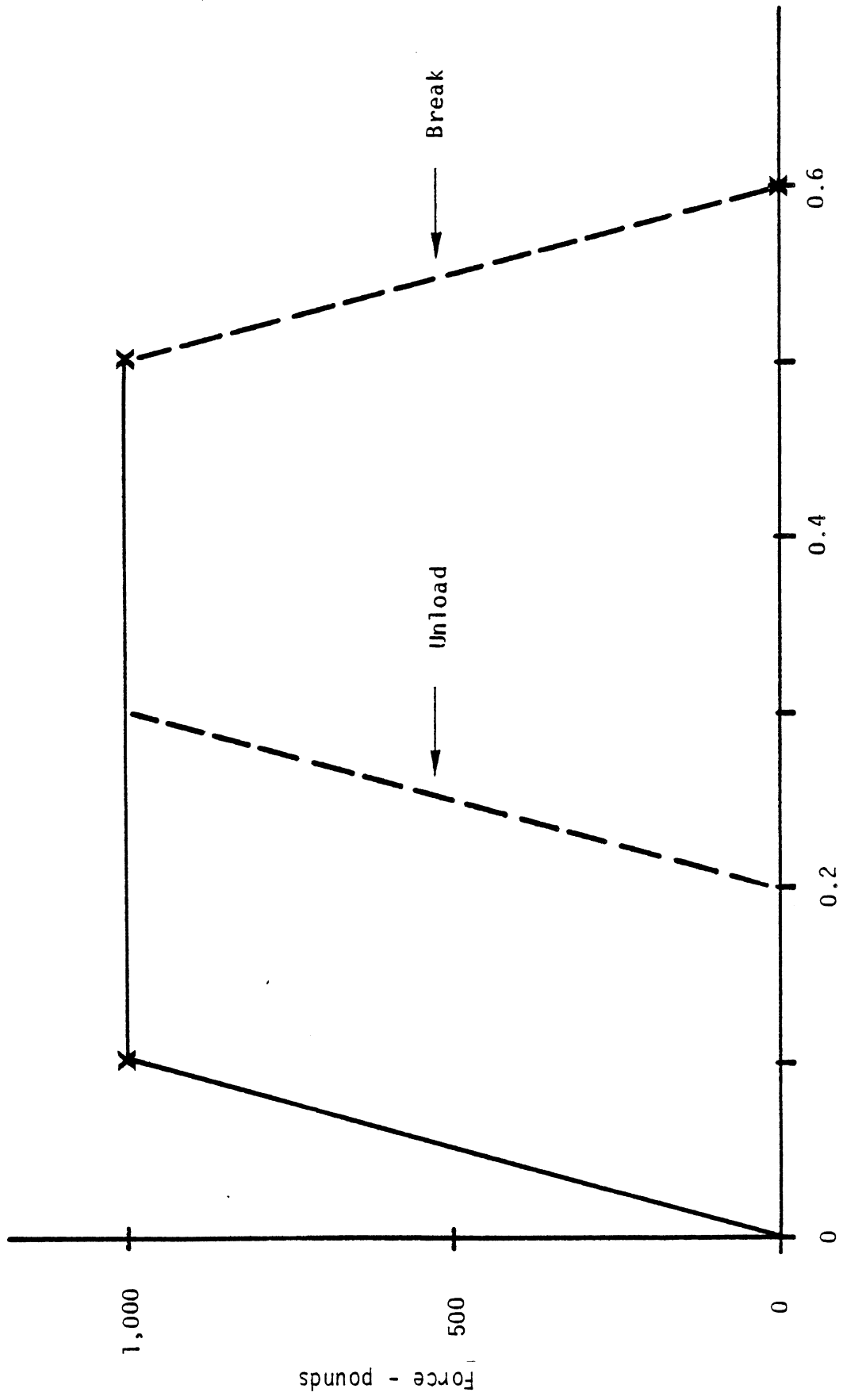
<u>Ellipsoid Name</u>	<u>Contact Panel on Ellipsoid Name</u>
Lower torso	Windshield
Lower torso	Hood
Lower torso	Grille Top
Upper torso	Roof
Upper torso	Windshield
Upper torso	Hood
Head	Roof
Head	Windshield
Head	Hood
Right upper leg	Hood
Right upper leg	Grille
Right upper leg	Grille Top
Right upper leg	Left upper leg
Right calf	Bumper
Right shin	Bumper
Right foot	Ground
Left upper leg	Hood
Left upper leg	Grille
Left upper leg	Grille Top
Left lower leg	Bumper
Left foot	Ground
Right upper arm	Hood
Right lower arm	Hood
Left upper arm	Hood
Left lower arm	Hood



x x x x Points
demonstrating fit
of polynomial to
tabular data.

$$F = 1000\delta - 562.5\delta^2 + 1031.25\delta^3 - 562.5\delta^4 + 93.75\delta^5$$

Figure 10. Panel force-deflection curve.



Deflection - inches
 Figure 11. Side window force-deflection curve

This is an idealization of data presented at the 11th Stapp Car Crash Conference by Siemonsen and Bruckner (7). It should be noted that tempered glass holds substantial force for a larger deformation than annealed or laminated glass due to its larger bending stiffness. It is presumed that the glass panel breaks upon reaching a deflection of 0.5 inch and behaves elastically until that deformation is reached.

The floor, seat back, and seat cushion are modeled as linear polynomials in force and deformation. The following coefficients were supplied with the original frontal impact data set by Calspan Corporation:

1. Seat back and seat cushion - 40 lb/in.
2. Floor - 860 lb/in.

4.1.1 Intrusion of Vehicle Components during Side Impact

Figure 12 shows the intrusion of the hip and door contact surfaces during the baseline side impact accident event. The overall motions of the vehicle take place in the coordinate system indicated in the figure. However, in the case of intrusion, the various components of the vehicle move and deform with respect to the vehicle. To represent this physically observed phenomena and to provide a realistic, but hypothetical, example for the baseline exercise, the arm rest and door are seen to begin intrusion at 5 ms and continue moving inward until 30 ms when they stop with respect to the remainder of the vehicle. Total intrusion is 5 inches. The software is capable of linear motion, as is the case used in this example, and also of panel rotation.

4.2 VEHICLE EXTERIOR FORCE-DEFORMATION CHARACTERISTICS

Three different force-deflection characteristic curves are used to define the properties of the seven contact surfaces which define the vehicle exterior and ground for pedestrian impact. All these curves are linear polynomials in deformation. The roof, windshield, hood, grille, and bumper have a coefficient of 1000 lb/in. The ground coefficient is 470 lb/in. The grille top surface was to be twice the average of the hood and grille, which is 2000 lb/in. The body ellipsoids are all as-

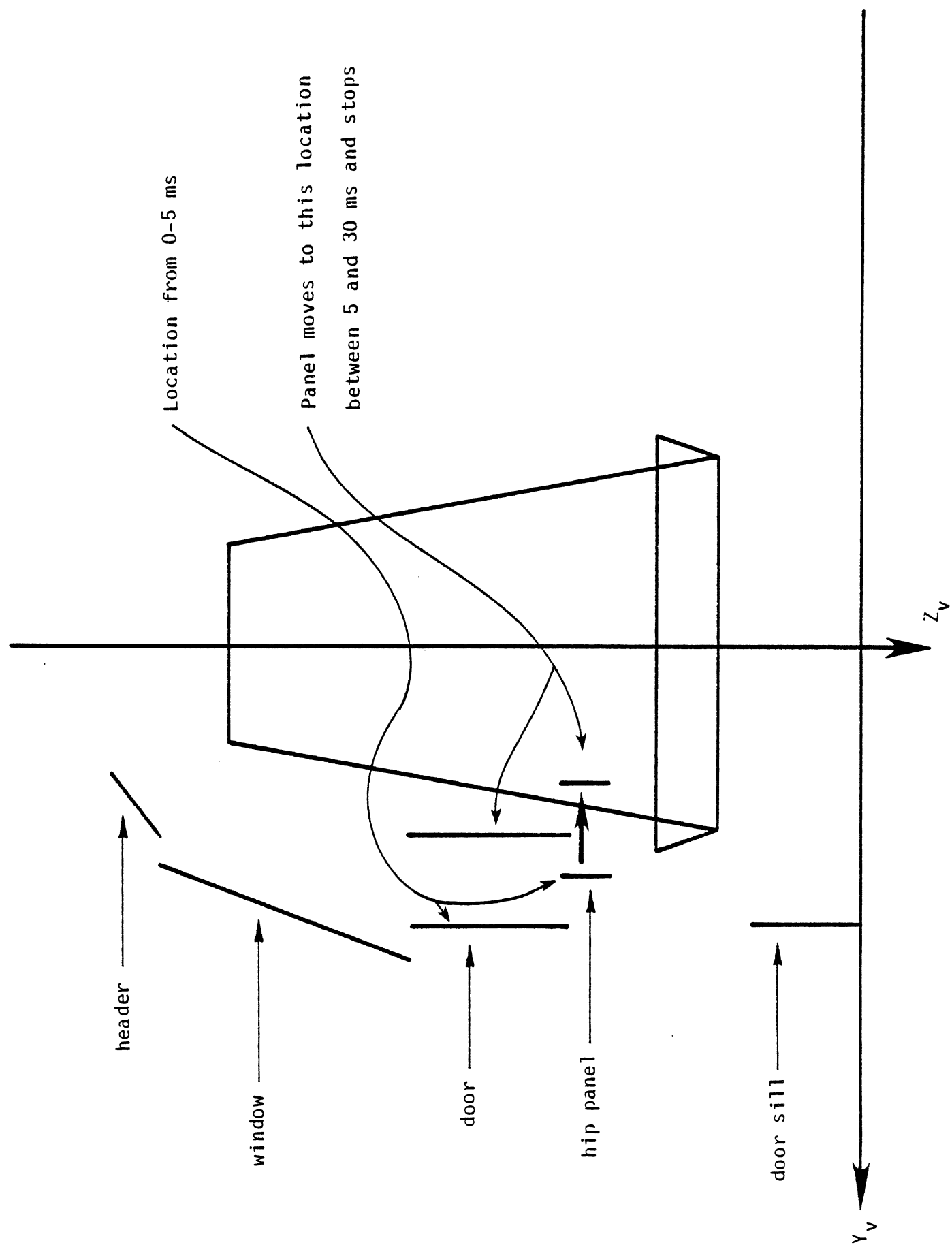


Figure 12. Intrusion of baseline hip panel and door contact surfaces during simulation.

sumed to be rigid. Any contact with the ground will also develop a tangential force to simulate sliding friction, the coefficient for which is 1.0.

These data are incomplete and represent only hypothetical estimates for the properties of a vehicle exterior. The data included in the Boeing Computer Services report by Karnes (3) are somewhat more complete but their sources are unknown. Particular problems exist with specifying both the stiffness and the energy absorbed in the various surfaces. Data from the Wayne State University project mentioned earlier are not available and the "Pedestrian Model Parametric Study" reports by Twigg and Tocher (8) contain values which may be unreasonably soft for current and advanced generation vehicles. It is recommended that the force-deformation data contained in this baseline be regarded as preliminary and that further work should be done to improve their quality.

5.0 THE COMPUTER EXERCISES

The purpose of this part of the report is to present the numerical details of the two baseline data sets and give summary details of the resulting computer exercises. For a complete copy of the simulation output it is necessary to exercise the data set or obtain a copy of the tape containing the exercise from MVMA or HSRI.

5.1 VEHICLE DECELERATIONS AND MOTIONS

The dynamics of the side impact simulation are initiated by forcing an acceleration of the occupant compartment. This causes the vehicle (and its contact surfaces) to begin to move with respect to inertial coordinates. Superimposed upon this movement is the prescribed intrusion of the side door hip contact panel with respect to the vehicle coordinate system. The occupant, initially at rest with respect to both inertial and vehicle coordinate systems, is carried along by the vehicle motions through impacts with the vehicle interior contact surfaces. The lateral acceleration profile applied to the vehicle is shown graphically in Figure 13.

The pedestrian impact is initiated by prescribing motions for the vehicle contact surfaces which are given an initial velocity of 10 mph and maintain this non-stop velocity throughout the simulation. The "vehicle coordinate system" remains motionless and coincident with the inertial coordinate system throughout the simulation. In other words, simulation of vehicle motions is accomplished by moving the vehicle contact surfaces as a unit with respect to the motionless "vehicle coordinate system." It should be noted that no motion was prescribed for the contact surface representing the ground. The reason for this unconventional approach to vehicle motion was to assure that the program output of pedestrian motions would be relative to inertial rather than vehicle coordinates, an option which was not available with the Calspan CVS at the time work started on the baseline simulations.

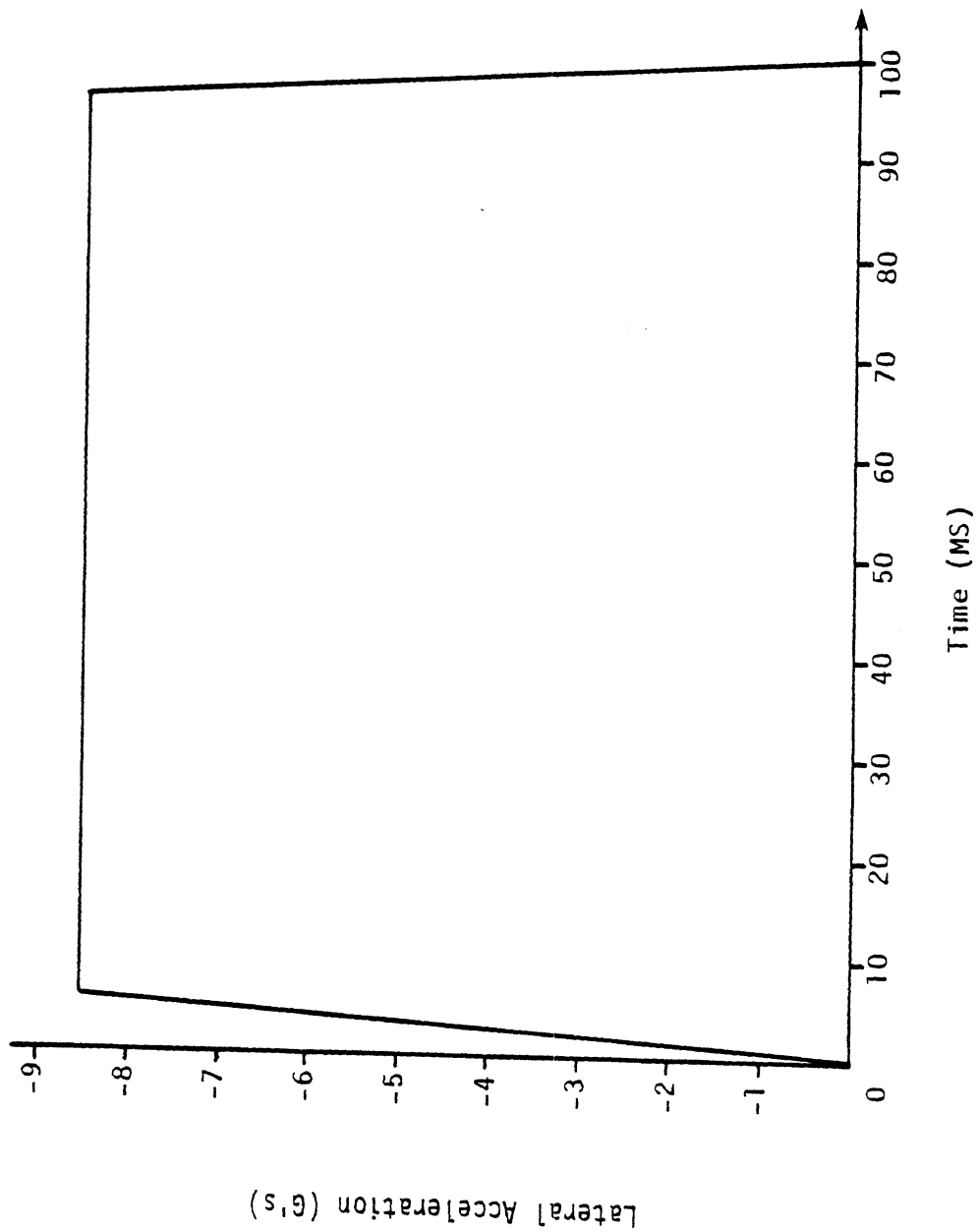


Fig. 13 Side Impact Vehicle Acceleration Curve.

5.2 SIDE IMPACT INPUT DATA

This part of the report contains the numerical details of the baseline side impact data set. Table 4 contains the computer-generated output of the input data set. Table 3 is a summary of the contents of this table to enable the reader to quickly find data quantities of interest. Table 5 is a copy of the baseline data file which was constructed for the exercise.

TABLE 3. CONTENTS OF OUTPUT OF INPUT TABLE (SIDE IMPACT)

Page in Table 4	Data Card I.D.	Input Quantities
1	A	Controls
2	B.2,B.3	Occupant mass and inertial properties. Joint definitions.
3	B.4,B.5	Joint torque characteristics.
4	B.6	Segment integration convergence test input.
5	C	Vehicle linear time histories.
6	C	Vehicle angular time histories.
7	D.2	Location of contact planes.
8	D.5	Ellipsoid semiaxes and orientation
8	D.7	Symmetry input
8	D.9.A	Material normal force specifications.
9,10	E.5.A-E.5.C.	Bivariate polynomial specifications for force generation
10	E.5.D-E.5.F,E.6	Bivariate table specifications for force generation
11	F.1	Allowed contacts
12	G.1,G.2,G.3	Initial Positions

CALSPAN 3-D CRASH VICTIM SIMULATION PROGRAM

CARDS A

31 MAR 1960
NPRI ARRAY

JUL 10, 1960
0 0 0 0 0 0 0 0 0 0

IRIN= 0
IRSOOT= 0
RSTIME = 0.0

BASLINE SIDE IMPACT LN DRIVER

UNITL = IN. UNITH = LB. UNITT = SEC.
GRAVITY VECTOR = (0.0 , 0.0 , 386.0880)

NDINT = 6 MSICPS = 100 DT = 0.001000 HW = 0.001000 HMAX = 0.005000 HMIN = 0.000500
KHTLPR= 1 MAXLIN= 501
EPSILONS 0.1000000000000000E-01 0.1000000000000000E-02 0.1000000000000000E+01 0.1000000000000000E+00 0.2000000000000000E+04 0.3000000000000000E+04

TABLE 4. Output of Baseline Input Data Set. Side Impact. (Page 1 of 12)

SEGMENT I SYM PLOT	MASS (LB.-SEC.**2/ IN.)	SEGMENT MOMENT OF INERTIA (LB.-SEC.**2- IN.)			X	Y	Z
		X	Y	Z			
1 LT 5	0.093	1.78000	1.14000	1.71000			
2 CT 4	0.024	0.32500	0.31400	0.14900			
3 UT 3	0.002	2.32000	1.65000	1.33000			
4 N 2	0.008	0.04000	0.04000	0.03660			
5 H 1	0.026	0.25900	0.31100	0.20000			
6 RUL 6	0.045	0.72700	0.70300	0.15400			
7 RLL 7	0.018	0.44000	0.44200	0.01900			
8 RF 8	0.007	0.03830	0.04340	0.01320			
9 LUL 9	0.045	0.72700	0.70300	0.15400			
10 LLL A	0.018	0.44000	0.44200	0.01900			
11 LF B	0.007	0.03830	0.04340	0.01320			
12 RUA C	0.014	0.16400	0.16600	0.01410			
13 RLA D	0.012	0.25500	0.25900	0.01150			
14 LUA E	0.014	0.16400	0.16600	0.01410			
15 LLA F	0.012	0.25500	0.25900	0.01150			

JOINT J SYM PLOT JNT PIN	LOCATION (IN.) - SEG (JNT)			LOCATION (IN.) - SEG (J+1)			PRIN. AXIS (DEG) - SEG (JNT)			PRIN. AXIS (DEG) - SEG (J+1)		
	X	Y	Z	X	Y	Z	YAW	PITCH	ROLL	YAW	PITCH	ROLL
1 P	1	-2	1	-1.50	0.0	2.50	0.0	0.0	0.0	0.0	0.0	0.0
2 W	0	-2	2	-1.50	0.0	6.80	0.0	0.0	0.0	0.0	0.0	0.0
3 NP	N	3	-2	0.0	0.0	3.80	0.0	0.0	0.0	0.0	0.0	0.0
4 MP	M	4	-2	0.0	0.0	3.30	0.0	0.0	0.0	0.0	0.0	0.0
5 RH	Q	1	0	2.10	4.45	2.50	0.0	0.0	0.0	0.0	0.0	5.72
6 RK	R	6	1	0.0	0.0	8.79	0.0	0.0	0.0	0.0	0.0	0.0
7 RA	S	7	-2	0.0	0.0	6.69	0.0	0.0	0.0	0.0	0.0	0.0
8 LH	T	1	0	2.10	-4.45	2.50	0.0	0.0	0.0	0.0	0.0	-5.72
9 LK	U	9	1	0.0	0.0	6.79	0.0	0.0	0.0	0.0	0.0	0.0
10 LA	V	10	-2	0.0	0.0	8.69	0.0	0.0	0.0	0.0	0.0	0.0
11 RS	W	3	-2	-0.80	7.60	-1.60	0.0	0.0	0.0	0.0	0.0	10.19
12 RE	X	12	-1	0.0	0.0	5.45	0.0	0.0	0.0	0.0	0.0	0.0
13 LS	Y	3	-2	-0.00	-7.60	-1.60	0.0	0.0	0.0	0.0	0.0	-10.19
14 LE	Z	14	-1	0.0	0.0	5.45	0.0	0.0	0.0	0.0	0.0	0.0

TABLE 4. Output of Baseline Input Data Set. Side Impact. (Page 2 of 12)

JOINT TORQUE CHARACTERISTICS

CARDS B.4

FLEXURAL SPRING CHARACTERISTICS

TORSIONAL SPRING CHARACTERISTICS

JOINT	SPRING COEF. (IN. LB./DEG**J)			ENERGY DISSIPATION COEF.			JOINT STOP (DEG)				
	LINEAR (J=1)	QUADRATIC (J=2)	CUBIC (J=3)	LINEAR (J=1)	QUADRATIC (J=2)	CUBIC (J=3)	LINEAR (J=1)	QUADRATIC (J=2)	CUBIC (J=3)		
1 P	209.440	609.230	0.0	1.000	5.000	5.000	343.830	609.230	0.0	1.000	5.000
2 W	20.944	60.923	0.0	1.000	35.000	35.000	34.383	60.923	0.0	1.000	35.000
3 MP	17.174	60.923	0.0	1.000	25.000	25.000	8.011	60.923	0.0	1.000	35.000
4 HP	21.293	60.923	0.0	1.000	25.000	25.000	8.011	60.923	0.0	1.000	35.000
5 RH	0.0	609.230	0.0	1.000	85.500	85.500	0.0	609.230	0.0	1.000	55.500
6 RK	0.0	16.754	0.0	1.000	58.300	58.300	0.0	0.0	0.0	0.0	0.0
7 RA	0.0	627.510	0.0	1.000	37.000	37.000	0.0	94.431	0.0	1.000	20.700
8 LH	0.0	609.230	0.0	1.000	85.500	85.500	0.0	609.230	0.0	1.000	55.500
9 LK	0.0	16.754	0.0	1.000	58.300	58.300	0.0	0.0	0.0	0.0	0.0
10 LA	0.0	627.510	0.0	1.000	37.000	37.000	0.0	94.431	0.0	1.000	20.700
11 RS	0.0	609.230	0.0	1.000	122.500	122.500	0.0	609.230	0.0	1.000	180.000
12 RE	0.0	11.697	0.0	1.000	65.300	65.300	0.0	0.0	0.0	0.0	0.0
13 LS	0.0	609.230	0.0	1.000	122.500	122.500	0.0	609.230	0.0	1.000	180.000
14 LE	0.0	11.697	0.0	1.000	65.300	65.300	0.0	0.0	0.0	0.0	0.0

CARDS B.5

JOINT VISCOUS CHARACTERISTICS AND LOCK-UNLOCK CONDITIONS

JOINT	VISCOUS COEFFICIENT (IN. LB.-SEC./DEG)		COULOMB FRICTION COEF. (IN. LB.)		FULL FRICTION ANGULAR VELOCITY (DEG/SEC.)		MAX TORQUE FOR A LOCKED JOINT (IN. LB.)		MIN TORQUE FOR UNLOCKED JOINT (IN. LB.)		MIN. ANG. VELOCITY FOR UNLOCKED JOINT (RAD/SEC.)		IMPULSE RESTITUTION COEFFICIENT
	1	2	1	2	1	2	1	2	1	2	1	2	
1 P	104.720	10.472	600.00	60.00	60.00	60.00	0.0	0.0	0.0	0.0	0.0	0.0	0.0
2 W	10.472	1.0472	60.00	6.00	60.00	60.00	0.0	0.0	0.0	0.0	0.0	0.0	0.0
3 MP	1.745	0.1745	10.00	1.00	60.00	60.00	0.0	0.0	0.0	0.0	0.0	0.0	0.0
4 HP	1.745	0.1745	10.00	1.00	60.00	60.00	0.0	0.0	0.0	0.0	0.0	0.0	0.0
5 RH	3.997	0.3997	229.00	22.90	60.00	60.00	0.0	0.0	0.0	0.0	0.0	0.0	0.0
6 RK	3.456	0.3456	193.00	19.30	60.00	60.00	0.0	0.0	0.0	0.0	0.0	0.0	0.0
7 RA	6.436	0.6436	25.00	2.50	60.00	60.00	0.0	0.0	0.0	0.0	0.0	0.0	0.0
8 LH	3.997	0.3997	229.00	22.90	60.00	60.00	0.0	0.0	0.0	0.0	0.0	0.0	0.0
9 LK	3.456	0.3456	193.00	19.30	60.00	60.00	0.0	0.0	0.0	0.0	0.0	0.0	0.0
10 LA	6.436	0.6436	25.00	2.50	60.00	60.00	0.0	0.0	0.0	0.0	0.0	0.0	0.0
11 RS	3.229	0.3229	185.00	18.50	60.00	60.00	0.0	0.0	0.0	0.0	0.0	0.0	0.0
12 RE	1.292	0.1292	74.00	7.40	60.00	60.00	0.0	0.0	0.0	0.0	0.0	0.0	0.0
13 LS	3.229	0.3229	185.00	18.50	60.00	60.00	0.0	0.0	0.0	0.0	0.0	0.0	0.0
14 LE	1.292	0.1292	74.00	7.40	60.00	60.00	0.0	0.0	0.0	0.0	0.0	0.0	0.0

TABLE 4. Output of Baseline Input Data Set. Side Impact. (Page 3 of 12)

SEGMENT INTEGRATION CONVERGENCE TEST INPUT

SEGMENT NO. SYM	ANGULAR VELOCITIES (RAD/SEC.)			LINEAR VELOCITIES (IN./SEC.)			ANGULAR ACCELERATIONS (RAD/SEC.**2)			LINEAR ACCELERATIONS (IN./SEC.**2)		
	MAG. TEST	ABS. ERROR	REL. ERROR	MAG. TEST	ABS. ERROR	REL. ERROR	MAG. TEST	ABS. ERROR	REL. ERROR	MAG. TEST	ABS. ERROR	REL. ERROR
1	LI	0.0	0.0	0.0	0.0	0.0	0.01	0.01	0.0100	0.00	0.00	0.0010
2	CI	0.0	0.0	0.0	0.0	0.0	0.01	0.01	0.0100	0.0	0.0	0.0
3	UT	0.0	0.0	0.0	0.0	0.0	0.01	0.01	0.0100	0.0	0.0	0.0
4	N	0.0	0.0	0.0	0.0	0.0	0.01	0.01	0.0100	0.0	0.0	0.0
5	II	0.0	0.0	0.0	0.0	0.0	0.01	0.01	0.0100	0.0	0.0	0.0
6	RUL	0.0	0.0	0.0	0.0	0.0	0.01	0.01	0.0100	0.0	0.0	0.0
7	RLL	0.0	0.0	0.0	0.0	0.0	0.01	0.01	0.0100	0.0	0.0	0.0
8	RF	0.0	0.0	0.0	0.0	0.0	0.01	0.01	0.0100	0.0	0.0	0.0
9	LUL	0.0	0.0	0.0	0.0	0.0	0.01	0.01	0.0100	0.0	0.0	0.0
10	LLL	0.0	0.0	0.0	0.0	0.0	0.01	0.01	0.0100	0.0	0.0	0.0
11	LF	0.0	0.0	0.0	0.0	0.0	0.01	0.01	0.0100	0.0	0.0	0.0
12	RUA	0.0	0.0	0.0	0.0	0.0	0.01	0.01	0.0100	0.0	0.0	0.0
13	RLA	0.0	0.0	0.0	0.0	0.0	0.01	0.01	0.0100	0.0	0.0	0.0
14	LUA	0.0	0.0	0.0	0.0	0.0	0.01	0.01	0.0100	0.0	0.0	0.0
15	LUA	0.0	0.0	0.0	0.0	0.0	0.01	0.01	0.0100	0.0	0.0	0.0

TABLE 4. Output of Baseline Input Data Set. Side Impact. (Page 4 of 12)

VEHICLE DECELERATION INPUTS												CARDS C			
DIRECT LATERAL IMPACT FROM REST															
YAW	PITCH	ROLL	XIPS	(VIPS) VTIME	ZIPS	XO(X)	XO(Y)	XO(Z)	NATAB	ATD	ADT				
0.0	0.0	0.0	0.0	0.0	0.0	0.0	0.0	0.0	-21	0.0	0.005000				
ROTATING VEHICLE LINEAR TIME HISTORY												PAGE NO. 1			
TIME (SEC.)	LINEAR DECELERATIONS (G'S)			LINEAR VELOCITIES (IN./SEC.)			LINEAR DISPLACEMENTS (IN.)								
	X	Y	Z	X	Y	Z	X	Y	Z	X	Y	Z			
0.0	0.0	0.0	0.0	0.0	0.0	0.0	0.0	0.0	0.0	0.0	0.0	0.0	0.0	0.0	0.0
0.00500	0.0	-0.500	0.0	-0.500	0.0	0.0	0.0	0.0	0.0	0.0	0.0	0.0	0.0	0.0	0.0
0.01000	0.0	-0.500	0.0	-0.500	0.0	0.0	0.0	0.0	0.0	0.0	0.0	0.0	0.0	0.0	0.0
0.01500	0.0	-0.500	0.0	-0.500	0.0	0.0	0.0	0.0	0.0	0.0	0.0	0.0	0.0	0.0	0.0
0.02000	0.0	-0.500	0.0	-0.500	0.0	0.0	0.0	0.0	0.0	0.0	0.0	0.0	0.0	0.0	0.0
0.02500	0.0	-0.500	0.0	-0.500	0.0	0.0	0.0	0.0	0.0	0.0	0.0	0.0	0.0	0.0	0.0
0.03000	0.0	-0.500	0.0	-0.500	0.0	0.0	0.0	0.0	0.0	0.0	0.0	0.0	0.0	0.0	0.0
0.03500	0.0	-0.500	0.0	-0.500	0.0	0.0	0.0	0.0	0.0	0.0	0.0	0.0	0.0	0.0	0.0
0.04000	0.0	-0.500	0.0	-0.500	0.0	0.0	0.0	0.0	0.0	0.0	0.0	0.0	0.0	0.0	0.0
0.04500	0.0	-0.500	0.0	-0.500	0.0	0.0	0.0	0.0	0.0	0.0	0.0	0.0	0.0	0.0	0.0
0.05000	0.0	-0.500	0.0	-0.500	0.0	0.0	0.0	0.0	0.0	0.0	0.0	0.0	0.0	0.0	0.0
0.05500	0.0	-0.500	0.0	-0.500	0.0	0.0	0.0	0.0	0.0	0.0	0.0	0.0	0.0	0.0	0.0
0.06000	0.0	-0.500	0.0	-0.500	0.0	0.0	0.0	0.0	0.0	0.0	0.0	0.0	0.0	0.0	0.0
0.06500	0.0	-0.500	0.0	-0.500	0.0	0.0	0.0	0.0	0.0	0.0	0.0	0.0	0.0	0.0	0.0
0.07000	0.0	-0.500	0.0	-0.500	0.0	0.0	0.0	0.0	0.0	0.0	0.0	0.0	0.0	0.0	0.0
0.07500	0.0	-0.500	0.0	-0.500	0.0	0.0	0.0	0.0	0.0	0.0	0.0	0.0	0.0	0.0	0.0
0.08000	0.0	-0.500	0.0	-0.500	0.0	0.0	0.0	0.0	0.0	0.0	0.0	0.0	0.0	0.0	0.0
0.08500	0.0	-0.500	0.0	-0.500	0.0	0.0	0.0	0.0	0.0	0.0	0.0	0.0	0.0	0.0	0.0
0.09000	0.0	-0.500	0.0	-0.500	0.0	0.0	0.0	0.0	0.0	0.0	0.0	0.0	0.0	0.0	0.0
0.09500	0.0	-0.500	0.0	-0.500	0.0	0.0	0.0	0.0	0.0	0.0	0.0	0.0	0.0	0.0	0.0
0.10000	0.0	-0.500	0.0	-0.500	0.0	0.0	0.0	0.0	0.0	0.0	0.0	0.0	0.0	0.0	0.0

TABLE 4. Output of Baseline Input Data Set. Side Impact. (Page 5 of 12)

TIME (SEC.)	ANGULAR ACCELERATIONS (DEG/SEC.**2)			ANGULAR VELOCITIES (DEG/SEC.)			ANGULAR DISPLACEMENTS		ROLL (DEG)
	X	Y	Z	X	Y	Z	YAW	PITCH	
0.0	0.0	0.0	0.0	0.0	0.0	0.0	0.0	0.0	0.0
0.00500	0.0	0.0	0.0	0.0	0.0	0.0	0.0	0.0	0.0
0.01000	0.0	0.0	0.0	0.0	0.0	0.0	0.0	0.0	0.0
0.01500	0.0	0.0	0.0	0.0	0.0	0.0	0.0	0.0	0.0
0.02000	0.0	0.0	0.0	0.0	0.0	0.0	0.0	0.0	0.0
0.02500	0.0	0.0	0.0	0.0	0.0	0.0	0.0	0.0	0.0
0.03000	0.0	0.0	0.0	0.0	0.0	0.0	0.0	0.0	0.0
0.03500	0.0	0.0	0.0	0.0	0.0	0.0	0.0	0.0	0.0
0.04000	0.0	0.0	0.0	0.0	0.0	0.0	0.0	0.0	0.0
0.04500	0.0	0.0	0.0	0.0	0.0	0.0	0.0	0.0	0.0
0.05000	0.0	0.0	0.0	0.0	0.0	0.0	0.0	0.0	0.0
0.05500	0.0	0.0	0.0	0.0	0.0	0.0	0.0	0.0	0.0
0.06000	0.0	0.0	0.0	0.0	0.0	0.0	0.0	0.0	0.0
0.06500	0.0	0.0	0.0	0.0	0.0	0.0	0.0	0.0	0.0
0.07000	0.0	0.0	0.0	0.0	0.0	0.0	0.0	0.0	0.0
0.07500	0.0	0.0	0.0	0.0	0.0	0.0	0.0	0.0	0.0
0.08000	0.0	0.0	0.0	0.0	0.0	0.0	0.0	0.0	0.0
0.08500	0.0	0.0	0.0	0.0	0.0	0.0	0.0	0.0	0.0
0.09000	0.0	0.0	0.0	0.0	0.0	0.0	0.0	0.0	0.0
0.09500	0.0	0.0	0.0	0.0	0.0	0.0	0.0	0.0	0.0
0.10000	0.0	0.0	0.0	0.0	0.0	0.0	0.0	0.0	0.0

TABLE 4. Output of Baseline Input Data Set. Side Impact. (Page 6 of 12)

PLANE NO.	1.	NUMTIM=	1.	NMATRL=	1.	LEGGSW=	3.	NINTRL=	16.	ISLAT=	0.	WITH NAME OF	HEADER
TIMEFF	0.0	X1	Y1	Z1	X2	Y2	Z2	X3	Y3	Z3			
		31.0000	0.0	-53.0000	-12.0000	0.0	-53.0000	31.0000	-10.5000	-41.0000			
PLANE NO.	2.	NUMTIM=	1.	NMATRL=	0.	LEGGSW=	3.	NINTRL=	16.	ISLAT=	0.	WITH NAME OF	WINDCH
TIMEFF	0.0	X1	Y1	Z1	X2	Y2	Z2	X3	Y3	Z3			
		31.0000	-9.0000	-50.0000	-12.0000	-9.0000	-50.0000	31.0000	-20.0000	-18.0000			
PLANE NO.	3.	NUMTIM=	1.	NMATRL=	4.	LEGGSW=	3.	NINTRL=	16.	ISLAT=	0.	WITH NAME OF	SLAT BACK
TIMEFF	0.0	X1	Y1	Z1	X2	Y2	Z2	X3	Y3	Z3			
		9.0000	-22.0000	0.0	-8.5000	-22.0000	-50.0000	9.0000	12.0000	0.0			
PLANE NO.	4.	NUMTIM=	1.	NMATRL=	4.	LEGGSW=	3.	NINTRL=	16.	ISLAT=	0.	WITH NAME OF	SEAT CUSHION
TIMEFF	0.0	X1	Y1	Z1	X2	Y2	Z2	X3	Y3	Z3			
		25.0000	-22.0000	-12.7500	0.0	-22.0000	-9.0000	25.0000	12.0000	-12.7500			
PLANE NO.	5.	NUMTIM=	1.	NMATRL=	3.	LEGGSW=	3.	NINTRL=	16.	ISLAT=	0.	WITH NAME OF	FLOOR
TIMEFF	0.0	X1	Y1	Z1	X2	Y2	Z2	X3	Y3	Z3			
		54.0000	-22.0000	0.0	0.0	-22.0000	0.0	54.0000	22.0000	0.0			
PLANE NO.	6.	NUMTIM=	1.	NMATRL=	1.	LEGGSW=	3.	NINTRL=	16.	ISLAT=	0.	WITH NAME OF	DOOR SILL
TIMEFF	0.0	X1	Y1	Z1	X2	Y2	Z2	X3	Y3	Z3			
		54.0000	-15.5000	-26.0000	0.0	-15.5000	-26.0000	54.0000	-15.5000	0.0			
PLANE NO.	7.	NUMTIM=	4.	NMATRL=	5.	LEGGSW=	3.	NINTRL=	16.	ISLAT=	0.	WITH NAME OF	DOOR
TIMEFF	0.0	X1	Y1	Z1	X2	Y2	Z2	X3	Y3	Z3			
		31.0000	-15.5000	-40.0000	-12.0000	-15.5000	-40.0000	31.0000	-15.5000	0.0			
	0.0050	31.0000	-15.5000	-40.0000	-12.0000	-15.5000	-40.0000	31.0000	-15.5000	0.0			
	0.0300	31.0000	-10.5000	-40.0000	-12.0000	-10.5000	-40.0000	31.0000	-10.5000	0.0			
	0.1000	31.0000	-10.5000	-40.0000	-12.0000	-10.5000	-40.0000	31.0000	-10.5000	0.0			
PLANE NO.	8.	NUMTIM=	4.	NMATRL=	1.	LEGGSW=	3.	NINTRL=	16.	ISLAT=	0.	WITH NAME OF	HIP PANEL
TIMEFF	0.0	X1	Y1	Z1	X2	Y2	Z2	X3	Y3	Z3			
		31.0000	-12.5000	-40.0000	-12.0000	-12.5000	-40.0000	31.0000	-12.5000	0.0			
	0.0050	31.0000	-12.5000	-40.0000	-12.0000	-12.5000	-40.0000	31.0000	-12.5000	0.0			
	0.0300	31.0000	-7.5000	-40.0000	-12.0000	-7.5000	-40.0000	31.0000	-7.5000	0.0			
	0.1000	31.0000	-7.5000	-40.0000	-12.0000	-7.5000	-40.0000	31.0000	-7.5000	0.0			

PLANE NO. 9, NDMTR= 1, NMATRL= 7, LEDDSM= 3, HINTRL= 16, ISOLAT= 0, WITH NAME OF B-PILLAR
 TIMEFF 0.0 X1 3.0000 Y1 -10.5000 Z1 -41.0000 X2 -12.0000 Y2 -10.5000 Z2 -41.0000 X3 3.0000 Y3 -15.5000 Z3 -26.0000

ADDITIONAL ELLIPSOID INPUT

CARDS 0.5

NO.	SEMIAXES (IN.)	OFFSET (IN.)	Z	ROTATION (DEG)	ROLL
	X Y Z	X Y Z		YAW PITCH	
1	4.940	6.940	7.600	0.0	0.0
2	4.910	6.350	7.030	0.0	0.0
3	4.410	6.780	4.940	0.0	0.0
4	2.570	2.380	3.280	0.0	0.0
5	3.950	3.100	4.590	0.0	0.0
6	2.950	3.740	12.400	0.0	0.0
7	2.300	2.230	9.070	0.0	0.0
8	1.520	1.800	5.220	0.0	0.0
9	2.990	3.740	12.400	0.0	0.0
10	2.300	2.230	9.070	0.0	0.0
11	1.520	1.800	5.220	0.0	0.0
12	2.070	1.640	6.880	0.0	0.0
13	1.300	1.110	8.380	0.0	0.0
14	2.070	1.640	6.880	0.0	0.0
15	1.300	1.110	8.380	0.0	0.0

BODY SEGMENT SYMMETRY INPUT

CARD 0.7

SFG NO. 1 2 3 4 5 6 7 8 9 10 11 12 13 14 15
 NSYM(J) 0 0 0 0 0 0 0 0 0 0 0 0 0 0 0

MATERIAL NORMAL FORCE SPECIFICATION

CARD 0.9.A

NMATRL	NAME	HSIW	HCK	TAB	IFRIK	DC	DE	DF	F SAT	DM
1	PAREL MATERIAL	1	-1	0	0.0	0.0	0.0	0.500000E+00	0.0	0.0
2	THORAX MATERIAL	-1	-1	0	0.0	0.0	0.0	0.500000E+00	0.0	0.0
3	FLOOR MATERIAL	-3	-1	0	0.0	0.0	0.0	0.500000E+00	0.0	0.0
4	SEAT MATERIAL	-2	-1	0	0.0	0.0	0.0	0.500000E+00	0.0	0.0
5	DOOR MATERIAL	-4	-1	0	0.0	0.0	0.0	0.500000E+00	0.0	0.0
6	GLASS MATERIAL	-5	1	0	0.0	0.0	0.0	0.500000E+00	0.100000E+04	0.100000E+05
7	PILLAR MATERIAL	-6	-1	0	0.0	0.0	0.0	0.600000E+00	0.0	0.0

BIVARIANT POLYNOMIAL SPECIFICATIONS

CARDS F.5.A-E.5.C

INPUT Y

COEFFICIENTS

TABLE 4. Output of Baseline Input Data Set. Side Impact. (Page 8 of 12)

1	0.4080000E+04	0.0	0.0	0.0	0.0	0.0	0.0	0.0	0.0
	0.0	0.0	0.0	0.0	0.0	0.0	0.0	0.0	0.0
	0.0	0.0	0.0	0.0	0.0	0.0	0.0	0.0	0.0
	0.0	0.0	0.0	0.0	0.0	0.0	0.0	0.0	0.0
2	0.4000000E+02	0.0	0.0	0.0	0.0	0.0	0.0	0.0	0.0
	0.0	0.0	0.0	0.0	0.0	0.0	0.0	0.0	0.0
	0.0	0.0	0.0	0.0	0.0	0.0	0.0	0.0	0.0
	0.0	0.0	0.0	0.0	0.0	0.0	0.0	0.0	0.0
3	0.8600000E+03	0.0	0.0	0.0	0.0	0.0	0.0	0.0	0.0
	0.0	0.0	0.0	0.0	0.0	0.0	0.0	0.0	0.0
	0.0	0.0	0.0	0.0	0.0	0.0	0.0	0.0	0.0
	0.0	0.0	0.0	0.0	0.0	0.0	0.0	0.0	0.0
4	0.1000000E+04	-0.5025000E+03	0.10312500E+04	-0.56250000E+03	0.93750000E+02	0.0	0.0	0.0	0.0
	0.0	0.0	0.0	0.0	0.0	0.0	0.0	0.0	0.0
	0.0	0.0	0.0	0.0	0.0	0.0	0.0	0.0	0.0
	0.0	0.0	0.0	0.0	0.0	0.0	0.0	0.0	0.0

TABLE 4. Output of Baseline Input Data Set. Side Impact. (Page 9 of 12)

BIVARIANT POLYNOMIAL SPECIFICATIONS

CARDS F.5.A-E.5.C

NPCLY	COEFFICIENTS			
5	0.1000000E+05	0.0	0.0	0.0
	0.0	0.0	0.0	0.0
	0.0	0.0	0.0	0.0
	0.0	0.0	0.0	0.0
	0.0	0.0	0.0	0.0
6	0.4000000E+04	0.0	0.0	0.0
	0.0	0.0	0.0	0.0
	0.0	0.0	0.0	0.0
	0.0	0.0	0.0	0.0
	0.0	0.0	0.0	0.0

BIVARIANT TABLE SPECIFICATIONS

CARDS E.5.D-E.5.F

NTABLE = 1	DEFL.	FORCE	DEFL.	FORCE	DEFL.	FORCE	DEFL.	FORCE	DEFL.	FORCE
0.0	0.	3.000	3000.	4.000	13000.					
G-R TABLE SPECIFICATIONS										
NTABLE	DEFLECTION	G RATIO	PK RATIO							
1	0.0	10000.0000	-1.0000	10000.0000	-1.0000	0.0	0.0	0.0	0.0	CARD E.6

TABLE 4. Output of Baseline Input Data Set. Side Impact. (Page 10 of 12)

ALLOWED CONTACTS AND ASSOCIATED FUNCTIONS			ELLIPSOID INDEX	ELLIPSOID NAME
ELLIPSOID INDEX	CONTACTS	PANEL INDEX OR NAME		
1	LOWER TORSO	3 SEAT BACK		
1	LOWER TORSO	4 SEAT CUSHION		
1	LOWER TORSO	3 HIP PANEL		
1	LOWER TORSO			
2	CENTER TORSO	3 SEAT BACK		
3	UPPER TORSO	3 SEAT BACK		
3	UPPER TORSO	7 DOOR		
5	HEAD	1 HEADER		
5	HEAD	2 WINDOW		
5	HEAD	2 B-PILLAR		
6	RIGHT UPPER LEG	4 SEAT CUSHION		
6	RIGHT UPPER LEG			
7	RIGHT LOWER LEG			
8	RIGHT FOOT	5 FLOOR		
8	RIGHT FOOT			
9	LEFT UPPER LEG	4 SEAT CUSHION		
9	LEFT UPPER LEG	8 HIP PANEL		
10	LEFT LOWER LEG	9 DOOR SILL		
11	LEFT FOOT	5 FLOOR		
11	LEFT FOOT	6 DOOR SILL		
14	LEFT UPPER ARM	9 B-PILLAR		
			13	RIGHT LOWER ARM
			9	LEFT UPPER LEG
			10	LEFT LOWER LEG
			11	LEFT FOOT

SUBROUTINE INITIAL INPUT

CARD 6.1

ZPLT(X) ZPLT(Y) ZPLT(Z) J1 J2 J3
 10.00 30.00 1.00 0 0 0

CARD 6.2

INITIAL POSITIONS (INERTIAL REFERENCE)

SEGMENT NO. SEG	LINEAR POSITION (IN.)			LINEAR VELOCITY (IN./SEC.)		
	X	Y	Z	X	Y	Z
1	LT	9.000000	0.00	-15.500000	0.00	0.00
2	CT	7.86263	0.00	-20.36995	0.00	0.00
3	UT	5.97063	0.00	-25.27109	0.00	0.00
4	N	3.84283	0.00	-34.95286	0.00	0.00
5	H	3.58319	0.00	-39.58322	0.00	0.00
6	RUL	18.54556	4.45000	-15.68940	0.00	0.00
7	KLL	29.41793	4.45000	-11.67975	0.00	0.00
8	RF	36.52826	4.45000	-4.64004	0.00	0.00
9	LUL	16.54556	-4.45000	-15.68970	0.00	0.00
10	LLL	29.41793	-4.45000	-11.67975	0.00	0.00
11	LF	36.52826	-4.45000	-4.64004	0.00	0.00
12	RUA	4.85545	7.60000	-25.41980	0.00	0.00
13	RLA	11.41041	7.60000	-19.39631	0.00	0.00
14	LUA	4.85545	-7.60000	-25.41980	0.00	0.00
15	LLA	11.41041	-7.60000	-19.39631	0.00	0.00

CARD 6.3

INITIAL ANGULAR ROTATION AND VELOCITY

SEGMENT NO. SEG	YAW	ANGULAR ROTATION (DEG)		ANGULAR VELOCITY (DEG/SEC.)		
		PITCH	ROLL	X	Y	Z
1	LT	0.00	12.00000	0.00	0.00	0.00
2	CT	0.00	12.00000	0.00	0.00	0.00
3	UT	0.00	12.00000	0.00	0.00	0.00
4	N	0.00	12.00000	0.00	0.00	0.00
5	H	0.00	12.00000	0.00	0.00	0.00
6	RUL	0.00	107.50000	0.00	0.00	0.00
7	KLL	0.00	107.50000	0.00	0.00	0.00
8	RF	0.00	107.50000	0.00	0.00	0.00
9	LUL	0.00	107.50000	0.00	0.00	0.00
10	LLL	0.00	36.00000	0.00	0.00	0.00
11	LF	0.00	190.00000	0.00	0.00	0.00
12	RUA	0.00	0.00	0.00	0.00	0.00
13	RLA	0.00	45.00000	0.00	0.00	0.00
14	LUA	0.00	0.00	0.00	0.00	0.00
15	LLA	0.00	85.00000	0.00	0.00	0.00

LINEAR AND ANGULAR VELOCITIES HAVE BEEN SET EQUAL TO THE INITIAL VEHICLE VELOCITIES.

TABLE 4. Output of Baseline Input Data Set. Side Impact. (Page 12 of 12)

LINE	DATE	DESCRIPTION	AMOUNT	DEBIT	CREDIT	BALANCE	ACCOUNT
1	31 MAR 1980	BASELINE SIDE IMPACT CN DRIVER	0.0000000	0.0000000	0.0000000	0.0000000	A.1.A
2							A.1.B
3							A.1.C
4		IN. LB-SEC.1.	1.0000000	0.0000000	0.0000000	386.088	A.3
5		6 100 0.001	0.005	0.00005	1.0000000	3000.	A.4
6		.01 .001	1.0000000	.1000000	2000.		A.5
7		0.0000000	.025	0.0000000	.100000000		A.6.A
8							A.6.B
9		15 14 SIERRA 292-1050-2004					B.1
10		LT 5.0925953	1.78	1.14	1.71		B.2
11		CT 4.0242949	0.325	0.314	0.149		B.2
12		UT 3.682235	2.32	1.65	1.33		B.2
13		N 2.6081069	0.04	0.04	0.0066		B.2
14		H 1.0262375	0.259	0.311	0.200		B.2
15		RUL 6.0451707	0.727	0.703	0.154		B.2
16		RLL 7.0180528	0.44	0.442	0.019		B.2
17		RF 8.0071227	0.0383	0.0434	0.0132		B.2
18		LUL 9.0451709	0.727	0.703	0.154		B.2
19		LLL A.0180528	0.44	0.442	0.019		B.2
20		LF B.0071227	0.0383	0.0434	0.0132		B.2
21		RUA C.0136238	0.164	0.166	0.0141		B.2
22		RLA D.0124064	0.255	0.259	0.0115		B.2
23		LUA E.0136238	0.164	0.166	0.0141		B.2
24		LLA F.0124064	0.255	0.259	0.0115		B.2
25		P 1 -2 -1.6	0.0	-2.5	-1.5	0.25	B.3.A
26		0.0	0.0	0.0	0.0	0.0	B.3.B
27		W 0 2 -2 -1.5	0.0	-2.3	-1.5	0.68	B.3.A
28		0.0	0.0	0.0	0.0	0.0	B.3.B
29		NP N 3 -2 -0.9	0.0	-2.2	0.0	3.8	B.3.A
30		0.0	0.0	0.0	0.0	0.0	B.3.B
31		HP M 4 -2 0.0	0.0	-1.2	-1.1	0.33	B.3.A
32		0.0	0.0	0.0	0.0	0.0	B.3.B
33		RH Q 1 0 2.1	4.45	2.5	0.0	-7.31	B.3.A
34		0.0	0.0	0.0	0.0	-66.50	B.3.B
35		RK R 6 1 0.0	0.0	6.79	0.0	-7.48	B.3.A
36		0.0	0.0	0.0	0.0	56.80	B.3.B
37		RA S 7 -2 0.0	0.0	8.69	1.54	-1.28	B.3.A
38		0.0	0.0	0.0	0.0	-81.00	B.3.B
39		LH T 1 0 2.1	-4.45	2.5	0.0	-7.31	B.3.A
40		0.0	0.0	0.0	0.0	-66.50	B.3.B
41		LK U 9 1 0.0	0.0	6.79	0.0	-7.48	B.3.A
42		0.0	0.0	0.0	0.0	56.80	B.3.B
43		LA V 10 -2 0.0	0.0	8.69	1.54	-1.28	B.3.A
44		0.0	0.0	0.0	0.0	-81.00	B.3.B
45		RS W 3 -2 -0.8	7.6	-1.6	0.0	-5.25	B.3.A
46		0.0	0.0	0.0	0.0	-57.50	B.3.B
47		RE X 12 -1 0.0	0.0	5.45	0.0	-6.58	B.3.A
48		0.0	0.0	0.0	0.0	-64.30	B.3.B
49		LS Y 3 -2 -0.8	-7.6	-1.6	0.0	-5.25	B.3.A
50		0.0	0.0	0.0	0.0	-57.50	B.3.B
51		LE Z 14 -1 0.0	0.0	5.45	0.0	-6.58	B.3.A
52		0.0	0.0	0.0	0.0	-64.30	B.3.B
53		209.44609.23	0.0	5.0	34.383609.23	0.0	B.4.A
54		20.94460.923	0.0	1.0	34.38360.923	0.0	B.4.A
55		17.17460.923	0.0	1.0	8.011160.923	0.0	B.4.A
56		21.29360.923	0.0	1.0	8.011160.923	0.0	B.4.A
57		.0 609.23	0.0	85.5	.0 609.23	0.0	B.4.A
58		.0 16.754	0.0	58.3	.0	0.0	B.4.A
59		.0 627.51	0.0	37.0	.0 94.431	0.0	B.4.A

	1	23	1.0	85.	61	3	.0	.0	5.5	1
61	.0	16.754	.0	58.3	.0	.0	.0	0.0	0.0	9 B.4.A
62	.0	627.51	.0	37.0	.0	94.431	.0	1.0	20.7	10 B.4.A
63	.0	609.23	.0	122.5	.0	609.23	.0	1.0	180.0	11 B.4.A
64	.0	11.697	.0	65.3	.0	.0	.0	0.0	0.0	12 B.4.A
65	.0	609.23	.0	122.5	.0	609.23	.0	1.0	180.0	13 B.4.A
66	.0	11.697	.0	65.3	.0	.0	.0	0.0	0.0	14 B.4.A
67	104.72	600.0	60.0							1 B.5.A
68	10.472	60.00	60.0							2 B.5.A
69	1.745	10.00	60.0							3 B.5.A
70	1.745	10.00	60.0							4 B.5.A
71	3.997	229.0	60.0							5 B.5.A
72	3.456	198.0	60.0							6 B.5.A
73	0.436	25.0	60.0							7 B.5.A
74	3.997	229.0	60.0							8 B.5.A
75	3.456	198.0	60.0							9 B.5.A
76	0.436	25.0	60.0							10 B.5.A
77	3.229	185.0	60.0							11 B.5.A
78	1.292	74.0	60.0							12 B.5.A
79	3.229	185.0	60.0							13 B.5.A
80	1.292	74.0	60.0							14 B.5.A
81					0.01	0.01	0.01	0.001	0.001	1 B.6
82					0.01	0.01	0.01			2 B.6
83					0.01	0.01	0.01			3 B.6
84					0.01	0.01	0.01			4 B.6
85					0.01	0.01	0.01			5 B.6
86					0.01	0.01	0.01			6 B.6
87					0.01	0.01	0.01			7 B.6
88					0.01	0.01	0.01			8 B.6
89					0.01	0.01	0.01			9 B.6
90					0.01	0.01	0.01			10 B.6
91					0.01	0.01	0.01			11 B.6
92					0.01	0.01	0.01			12 B.6
93					0.01	0.01	0.01			13 B.6
94					0.01	0.01	0.01			14 B.6
95					0.01	0.01	0.01			15 B.6
96										C.1
97	0.0	0.0	0.0	0.0	0.0	0.0	0.0	-21	0.0	0.005
98	0.	0.	0.	0.	0.	0.	0.	0.	0.	1 C.4
99	0.	0.	0.	0.	0.	0.	0.	0.	0.	2 C.4
100	0.	0.	0.	0.	0.	0.	0.	0.	0.	3 C.4
101	0.	0.	0.	0.	0.	0.	0.	0.	0.	4 C.4
102	0.	0.	0.	0.	0.	0.	0.	0.	0.	5 C.4
103	0.	0.	0.	0.	0.	0.	0.	0.	0.	6 C.4
104	0.	0.	0.	0.	0.	0.	0.	0.	0.	7 C.4
105	0.	0.	0.	0.	0.	0.	0.	0.	0.	8 C.4
106	0.	0.	0.	0.	0.	0.	0.	0.	0.	9 C.4
107	0.	0.	0.	0.	0.	0.	0.	0.	0.	10 C.4
108	0.	0.	0.	0.	0.	0.	0.	0.	0.	11 C.4
109	0.	0.	0.	0.	0.	0.	0.	0.	0.	12 C.4
110	0.	0.	0.	0.	0.	0.	0.	0.	0.	13 C.4
111	0.	0.	0.	0.	0.	0.	0.	0.	0.	14 C.4
112	0.	0.	0.	0.	0.	0.	0.	0.	0.	15 C.4
113	0.	0.	0.	0.	0.	0.	0.	0.	0.	16 C.4
114	0.	0.	0.	0.	0.	0.	0.	0.	0.	17 C.4
115	0.	0.	0.	0.	0.	0.	0.	0.	0.	18 C.4
116	0.	0.	0.	0.	0.	0.	0.	0.	0.	19 C.4
117	0.	0.	0.	0.	0.	0.	0.	0.	0.	20 C.4
118	0.	0.	0.	0.	0.	0.	0.	0.	0.	21 C.4
119	9	0	0	15	0	7	0	.1	.0001	1

DIRECT LATERAL IMPACT FROM REST

97	0.0	0.0	0.0	0.0	0.0	0.0	0.0	0.0	0.0	0.005
98	0.	0.	0.	0.	0.	0.	0.	0.	0.	1 C.4
99	0.	0.	0.	0.	0.	0.	0.	0.	0.	2 C.4
100	0.	0.	0.	0.	0.	0.	0.	0.	0.	3 C.4
101	0.	0.	0.	0.	0.	0.	0.	0.	0.	4 C.4
102	0.	0.	0.	0.	0.	0.	0.	0.	0.	5 C.4
103	0.	0.	0.	0.	0.	0.	0.	0.	0.	6 C.4
104	0.	0.	0.	0.	0.	0.	0.	0.	0.	7 C.4
105	0.	0.	0.	0.	0.	0.	0.	0.	0.	8 C.4
106	0.	0.	0.	0.	0.	0.	0.	0.	0.	9 C.4
107	0.	0.	0.	0.	0.	0.	0.	0.	0.	10 C.4
108	0.	0.	0.	0.	0.	0.	0.	0.	0.	11 C.4
109	0.	0.	0.	0.	0.	0.	0.	0.	0.	12 C.4
110	0.	0.	0.	0.	0.	0.	0.	0.	0.	13 C.4
111	0.	0.	0.	0.	0.	0.	0.	0.	0.	14 C.4
112	0.	0.	0.	0.	0.	0.	0.	0.	0.	15 C.4
113	0.	0.	0.	0.	0.	0.	0.	0.	0.	16 C.4
114	0.	0.	0.	0.	0.	0.	0.	0.	0.	17 C.4
115	0.	0.	0.	0.	0.	0.	0.	0.	0.	18 C.4
116	0.	0.	0.	0.	0.	0.	0.	0.	0.	19 C.4
117	0.	0.	0.	0.	0.	0.	0.	0.	0.	20 C.4
118	0.	0.	0.	0.	0.	0.	0.	0.	0.	21 C.4

TABLE 5. Listing of Baseline Side Impact Input Data File (Page 2 of 6)

120	1	1	3	16	0	HEADER				
121	0.	31.				0.0	-53.	D.2.A		
122		-12.				0.0	-53.	A1 D.2.B		
123		31.				-10.5	-41.	A1 D.2.C		
124	2	1	6	3	16	0	WINDOW	A1 D.2.D		
125	0.	31.0				-9.0	-50.	D.2.A		
126		-12.				-9.0	-50.	B1 D.2.B		
127		31.0				-20.0	-18.	B1 D.2.C		
128	3	1	4	3	16	0	SEAT BACK	B1 D.2.D		
129	0.	9.				-22.0	0.	D.2.A		
130		-8.5				-22.0	-50.	C1 D.2.B		
131		9.				12.0	0.	C1 D.2.C		
132	4	1	4	3	16	0	SEAT CUSHION	C1 D.2.D		
133	0.	25.				-22.0	-12.75	D1 D.2.A		
134		0.				-22.0	-9.	D1 D.2.B		
135		25.				12.0	-12.75	D1 D.2.C		
136	5	1	3	3	16	0	FLOOR	D1 D.2.D		
137	0.	54.				-22.0	0.0	D.2.A		
138		0.				-22.0	0.0	E1 D.2.B		
139		54.0				22.0	0.0	E1 D.2.C		
140	6	1	1	3	16	0	DOOR SILL	E1 D.2.D		
141	0.	54.0				-15.5	-26.	D.2.A		
142		0.0				-15.5	-26.	F1 D.2.B		
143		54.				-15.5	0.	F1 D.2.C		
144	7	4	5	3	16	0	DOOR	F1 D.2.D		
145	0.	31.				-15.5	-40.	D.2.A		
146		-12.				-15.5	-40.	G1 D.2.B		
147		31.				-15.5	0.	G1 D.2.C		
147.1	.005	31.				-15.5	-40.	G1 D.2.D		
147.2		-12.				-15.5	-40.	G2 D.2.B		
147.3		31.				-15.5	0.	G2 D.2.C		
147.4	.03	31.				-10.5	-40.	G2 D.2.D		
147.5		-12.				-10.5	-40.	G3 D.2.B		
147.6		31.				-10.5	0.	G3 D.2.C		
147.7	.1	31.				-10.5	-40.	G3 D.2.D		
147.8		-12.				-10.5	-40.	G4 D.2.B		
147.9		31.				-10.5	0.	G4 D.2.C		
148	8	4	1	3	16	0	HIP PANEL	G4 D.2.D		
149	0.	31.				-12.5	-40.	D.2.A		
150		-12.				-12.5	-40.	H1 D.2.B		
151		31.				-12.5	0.	H1 D.2.C		
152	.005	31.				-12.5	-40.	H1 D.2.D		
153		-12.				-12.5	-40.	H2 D.2.B		
154		31.				-12.5	0.	H2 D.2.C		
155	.03	31.				-7.5	-40.	H2 D.2.D		
156		-12.				-7.5	-40.	H3 D.2.B		
157		31.				-7.5	0.	H3 D.2.C		
158	.1	31.				-7.5	-40.	H3 D.2.D		
159		-12.				-7.5	-40.	H4 D.2.B		
160		31.				-7.5	0.	H4 D.2.C		
160.2	9	1	7	3	16	0	B-PILLAR	H4 D.2.D		
160.4	0.	3.				-10.5	-41.	D.2.A		
160.6		-12.				-10.5	-41.	I1 D.2.B		
160.8		3.				-15.5	-26.	I1 D.2.C		
161	1	1	0	LOWER	TORSO	4.94	6.94	7.6	0.	I1 D.2.D
162	2	2	0	CENTER	TORSO	4.91	6.35	7.03	0.	0.5
163	3	3	2	UPPER	TORSO	4.41	6.78	4.94	0.	0.5
164	4	4	0	NECK		2.57	3.38	3.28	0.	0.5
165	5	5	0	HEAD		3.99	3.1	4.59	0.	0.5
166	6	6	0	RIGHT	UPPER LEG	2.99	3.74	12.4	0.	0.5

222	6 -9								F.1.1.B
223	7 1								F.1.1.A
224	7 -10								F.1.1.B
225	8 2								F.1.1.A
226	8 5								F.1.1.B
227	8 -11								F.1.1.B
228	9 2								F.1.1.A
229	9 4								F.1.1.B
230	9 8								F.1.1.B
231	10 1								F.1.1.A
232	10 6								F.1.1.B
233	11 2								F.1.1.A
234	11 5								F.1.1.B
235	11 6								F.1.1.B
236	12 0								F.1.1.A
237	13 0								F.1.1.A
238	14 1								F.1.1.A
238.5	14 9								F.1.1.B
239	15 0								F.1.1.A
240									F.1.1.A
241	10.0	30.0	1.0	0					G.1
242	9.	0.0	-15.5						1 G.2
243	0.0	12.0	0.0						1 G.3
244	0.0	12.0	0.0						2 G.3
245	0.0	12.0	0.0						3 G.3
246	0.0	12.0	0.0						4 G.3
247	0.0	12.0	0.0						5 G.3
248	0.0	107.5	0.0						6 G.3
249	0.0	36.0	0.0						7 G.3
250	0.0	140.0	0.0						8 G.3
251	0.0	107.5	0.0						9 G.3
252	0.0	36.0	0.0						10 G.3
253	0.0	140.0	0.0						11 G.3
254	0.0	0.0	0.0						12 G.3
255	0.0	85.0	0.0						13 G.3
256	0.0	0.0	0.0						14 G.3
257	0.0	85.0	0.0						15 G.3
258	11		0.0	0.0	0.0	0.0	0.0		H.1.1.A
259	3		0.0	0.0	0.0	0.0	0.0		2 H.1.1.B
260	5		0.0	0.0	0.0	0.0	0.0		3 H.1.1.B
261	6		0.0	0.0	0.0	0.0	0.0		4 H.1.1.B
262	8								5 H.1.1.B
263	9								6 H.1.1.B
264	11								7 H.1.1.B
265	12		0.0	0.0	0.0	0.0	0.0		8 H.1.1.B
266	13								9 H.1.1.B
267	14								10 H.1.1.B
268	15								11 H.1.1.B
269	0								H.2.A
270	11		0.0	0.0	0.0	0.0	0.0		H.3.A
271	3		0.0	0.0	0.0	0.0	0.0		2 H.3.B
272	5		0.0	0.0	0.0	0.0	0.0		3 H.3.B
273	6		0.0	0.0	0.0	0.0	0.0		4 H.3.B
274	8								5 H.3.B
275	9								6 H.3.B
276	11								7 H.3.B
277	12		0.0	0.0	0.0	0.0	0.0		8 H.3.B
278	13								9 H.3.B
279	14								10 H.3.B
280	15								11 H.3.B

TABLE 5. Listing of Baseline Side Impact Input Data File (Page 5 of 5)

281	11	1	3	5	6	8	9	11	12	13	14	15	H.4.A
282	0												H.5.A
283	11	1	3	5	6	8	9	11	12	13	14	15	H.6.A
284	14	1	2	3	4	5	8	6	9	7	10	11	H.7.A
285		13	12	14									H.7.B

END OF FILE

TABLE 5. Listing of Baseline Side Impact Input Data File (Page 6 of 6)

5.3 PEDESTRIAN IMPACT INPUT DATA

This part of the report contains the numerical details of the baseline pedestrian impact data set. Table 7 contains the computer-generated output of the input data set. Table 6 is a summary of the contents of this table. Table 8 is a copy of the baseline data file which was constructed for this exercise.

TABLE 6. CONTENTS OF OUTPUT OF INPUT TABLE. PEDESTRIAN IMPACT.

Page in Table 7	Data Card I.D.	Input Quantities
1	A	Controls
2	B.2,B.3	Occupant mass and inertial properties. Joint definitions.
3	B.4,B.5	Joint torque characteristics.
4	B.6	Segment integration convergence test input.
5	C	Vehicle linear and angular time histories.
6	D.2	Location of contact planes.
7	D.5	Ellipsoid semiaxes and orientation
7	D.7	Symmetry input
7	D.9.A	Material normal force specifications.
7	D.9.B	Material tangential force specifications.
7,8	E.5.A-E.5.C	Bivariate polynomial specifications for force generation
9	F.1	Allowed contacts
10	G.1,G.2,G.3	Initial positions

The Tables 6-8 have described the pedestrian data set for the case of a simple hinge knee. Some modifications were necessary to simulate the hinge knee with the capability of breakage using the Euler joint option as was discussed in Part 3.2. Changes were necessary to the B.3, B.4, and B.5 cards. Table 9 contains the new or changed lines (marked with an asterisk) in the data listing surrounded by unchanged lines for comparison with Table 8.

CALSPAN 3-D CRASH VICTIM SIMULATION PROGRAM

17 APR 1980 OCT 1, 1980 IRSIN= 0 IRSOUT= 0 PSTIME = 0.0
 NPRT ARRAY 1 0 0 0 0 0 0 1 1 0

CARD 5 A

BASELINE PEDESTRIAN DATA SET

UNIT = IN. UNITF = LB. UNIT = SEC.
 GRAVITY VECTOR = (0.0 , 0.0 , 386.0880) 0.100000000E+01 0.100000000E+01 0.100000000E+01
 NDINT = 4 NSTEPS = 200 DT = 0.005000 H0 = 0.005000 HMAX = 0.005000 HMIN = 0.005000
 KNTLPR= 1 MAXLIN= 501
 EPSILONS 0.100000000000E-01 0.100000000000E-02 0.100000000000E+01 0.100000000000E+00 0.500000000000E+00 0.600000000000E+03

TABLE 7. Output of Baseline Input Data Set. Pedestrian Impact. (Page 1 of 10)

CRASH VICTIM MODIFIED SIERRA 18 SEGMENTS 17 JOINTS

I	SYM	PLCT	SEGMENT	MASS			SEGMENT MOMENT OF INERTIA			X	Y	Z
				(LB.-SEC.**2/ IN.)	(LB.-SEC.**2/ IN.)	(LB.-SEC.**2/ IN.)	(LB.-SEC.**2 - IN.)	(LB.-SEC.**2 - IN.)	(LB.-SEC.**2 - IN.)			
1	LT	5		0.093	1.78000	1.14000	1.71000					
2	CT	4		0.024	0.32500	0.31400	0.14900					
3	UT	3		0.082	2.32000	1.65000	1.33000					
4	U	2		0.008	0.04000	0.04000	0.09660					
5	A	1		0.026	0.25900	0.31100	0.20000					
6	RUL	6		0.045	0.72700	0.74300	0.15400					
7	URLL	7		0.004	0.00660	0.00663	0.00410					
8	LRL	7		0.014	0.21480	0.21578	0.01490					
9	RF	8		0.007	0.03830	0.04340	0.01320					
10	LUL	9		0.045	0.72700	0.74300	0.15400					
11	LLL	A		0.018	0.44000	0.44200	0.01900					
12	LF	B		0.007	0.03830	0.04340	0.01320					
13	RUA	C		0.014	0.16400	0.16600	0.01410					
14	RLA	D		0.008	0.20000	0.20000	0.01000					
15	LUA	E		0.014	0.16400	0.16600	0.01410					
16	LUA	F		0.008	0.20000	0.20000	0.01000					
17	RHA	G		0.005	0.10000	0.10000	0.01070					
18	LHA	H		0.005	0.10000	0.10000	0.01000					

J	SYM	PLOT	JNT	PIN	LOCATION(IN.) - SEG(JNT)			LOCATION(IN.) - SEG(J+1)			PRIN. AXIS(DEG) - SEG(JNT)	PRIN. AXIS(DEG) - SEG(J+1)	YAW	PITCH	ROLL
					X	Y	Z	X	Y	Z					
1	P		1	-2	-1.60	0.0	-2.50	-1.50	0.0	2.50	0.0	0.0	0.0	0.0	
2	M		2	-2	-1.50	0.0	-2.30	-1.50	0.0	6.80	0.0	0.0	0.0	0.0	
3	NP		3	-2	-0.90	0.0	-2.20	0.0	0.0	3.80	0.0	0.0	0.0	0.0	
4	MP		4	-2	0.0	0.0	-1.20	-1.10	0.0	3.30	0.0	0.0	0.0	0.0	
5	RH		5	0	0.0	2.80	1.50	0.0	0.0	-7.31	0.0	0.0	0.0	0.0	
6	RK		6	1	0.0	0.0	6.79	0.0	0.0	-1.75	0.0	0.0	0.0	0.0	
7	RTF		7	-2	0.0	0.0	1.75	0.0	0.0	-6.33	0.0	0.0	0.0	0.0	
8	RA		8	-2	0.0	0.0	6.33	1.54	0.0	-1.28	0.0	0.0	0.0	0.0	
9	LH		9	0	0.0	-2.80	1.50	0.0	0.0	-7.31	0.0	0.0	0.0	0.0	
10	LK		10	1	0.0	0.0	6.79	0.0	0.0	-7.48	0.0	0.0	0.0	0.0	
11	LA		11	-2	0.0	0.0	8.69	1.54	0.0	-1.28	0.0	0.0	0.0	0.0	
12	RS		12	-2	1.00	6.60	-1.60	0.0	0.0	-5.25	0.0	0.0	0.0	0.0	
13	RL		13	-1	0.0	0.0	5.45	0.0	0.0	-4.00	0.0	0.0	0.0	0.0	
14	LS		14	-2	1.00	-6.60	-1.60	0.0	0.0	-5.25	0.0	0.0	0.0	0.0	
15	LE		15	-1	0.0	0.0	5.45	0.0	0.0	-4.00	0.0	0.0	0.0	0.0	
16	RW		16	-1	0.0	0.0	4.00	0.0	0.0	-2.00	0.0	0.0	0.0	0.0	
17	LW		17	-1	0.0	0.0	4.00	0.0	0.0	-2.00	0.0	0.0	0.0	0.0	

CARDS B.3

TABLE 7. Output of Baseline Input Data Set. Pedestrian Impact. (Page 2 of 10)

JOINT TORQUE CHARACTERISTICS

CARDS R.4

FLEXURAL SPRING CHARACTERISTICS

TORSIONAL SPRING CHARACTERISTICS

JOINT	FLEXURAL SPRING CHARACTERISTICS			TORSIONAL SPRING CHARACTERISTICS			ENERGY DISSIPATION COEF.	JOINT STOP (DEG)
	SPRING COEF. (IN. LB./DEG**J) LINEAR (J=1)	QUADRATIC (J=2)	CUBIC (J=3)	SPRING COEF. (IN. LB./DEG**J) LINEAR (J=1)	QUADRATIC (J=2)	CUBIC (J=3)		
1 P	10.000	609.230	0.0	10.000	609.230	0.0	1.000	20.000
2 W	20.944	60.923	0.0	34.383	60.923	0.0	1.000	35.000
3 HP	17.174	60.923	0.0	8.011	60.923	0.0	1.000	35.000
4 HP	21.293	60.923	0.0	8.011	60.923	0.0	1.000	35.000
5 RH	0.0	609.230	0.0	0.0	609.230	0.0	1.000	70.000
6 RK	0.0	16.754	0.0	0.0	1000.000	0.0	1.000	90.000
7 RTF	0.0	0.0	0.0	0.0	0.0	0.0	1.000	0.0
8 RA	0.0	627.510	0.0	0.0	94.431	0.0	1.000	70.700
9 LH	0.0	609.230	0.0	0.0	609.230	0.0	1.000	70.500
10 LK	0.0	16.754	0.0	0.0	1000.000	0.0	1.000	90.000
11 LA	0.0	627.510	0.0	0.0	94.431	0.0	1.000	90.700
12 RS	0.0	609.230	0.0	0.0	609.230	0.0	1.000	190.000
13 RE	0.0	11.697	0.0	0.0	1000.000	0.0	1.000	90.000
14 LS	0.0	609.230	0.0	0.0	609.230	0.0	1.000	190.000
15 LE	0.0	11.697	0.0	0.0	1000.000	0.0	1.000	90.000
16 RW	0.0	600.000	0.0	0.0	600.000	0.0	1.000	90.000
17 LW	0.0	600.000	0.0	0.0	600.000	0.0	1.000	90.000

CARDS R.5

JOINT VISCOUS CHARACTERISTICS AND LOCK-UNLOCK CONDITIONS

JOINT	VISCOUS COEFFICIENT (IN. LB.SEC./DEG)	COULOMB FRICTION (IN. LB.)	FULL FRICTION ANGULAR VELOCITY (DEG/SEC.)	MAX TORQUE FOR A LOCKED JOINT (IN. LB.)	MIN TORQUE FOR UNLOCKED JOINT (IN. LB.)	MEM. ANG. VELOCITY FOR UNLOCKED JOINT (RAD/SEC.)	IMPULSE RESTITUTION COEFFICIENT
2 W	10.472	10.00	30.00	0.0	0.0	0.0	0.0
3 HP	1.745	10.00	30.00	0.0	0.0	0.0	0.0
4 HP	1.745	10.00	30.00	0.0	0.0	0.0	0.0
5 RH	3.997	10.00	30.00	0.0	0.0	0.0	0.0
6 RK	1.000	10.00	30.00	0.0	0.0	0.0	0.0
7 RTF	0.0	0.0	1.00	505.50	0.0	0.0	0.0
8 RA	0.416	10.00	30.00	0.0	0.0	0.0	0.0
9 LH	3.997	10.00	30.00	0.0	0.0	0.0	0.0
10 LK	1.000	10.00	30.00	0.0	0.0	0.0	0.0
11 LA	0.436	10.00	30.00	0.0	0.0	0.0	0.0
12 RS	0.0	0.0	30.00	0.0	0.0	0.0	0.0
13 RE	0.200	10.00	30.00	0.0	0.0	0.0	0.0
14 LS	0.0	0.0	30.00	0.0	0.0	0.0	0.0
15 LE	0.300	50.00	30.00	0.0	0.0	0.0	0.0
16 RW	1.000	100.00	30.00	0.0	0.0	0.0	0.0
17 LW	1.000	100.00	30.00	0.0	0.0	0.0	0.0

TABLE 7. Output of Baseline Input Data Set. Pedestrian Impact. (Page 3 of 10)

VEHICLE DECELERATION COEFFICIENT TEST INPUT												
SEQUENT NO. SYM	ANGULAR VELOCITIES (RAD/SEC.)			LINEAR VELOCITIES (IN./SEC.)			ANGULAR ACCELERATIONS (RAD/SEC.**2)			LINEAR ACCELERATIONS (IN./SEC.**2)		
	MAG- TEST	ABS- ERROR	REL- ERROR	MAG- TEST	ABS- ERROR	REL- ERROR	MAG- TEST	ABS- ERROR	REL- ERROR	MAG- TEST	ABS- ERROR	REL- ERROR
1	LF	0.0	0.0	0.0	0.0	0.0	0.0	0.0	0.0	0.0	0.0	0.0
2	CF	0.0	0.0	0.0	0.0	0.0	0.0	0.0	0.0	0.0	0.0	0.0
3	RT	0.0	0.0	0.0	0.0	0.0	0.0	0.0	0.0	0.0	0.0	0.0
4	N	0.0	0.0	0.0	0.0	0.0	0.0	0.0	0.0	0.0	0.0	0.0
5	H	0.0	0.0	0.0	0.0	0.0	0.0	0.0	0.0	0.0	0.0	0.0
6	RUL	0.0	0.0	0.0	0.0	0.0	0.0	0.0	0.0	0.0	0.0	0.0
7	URLL	0.0	0.0	0.0	0.0	0.0	0.0	0.0	0.0	0.0	0.0	0.0
8	LRL	0.0	0.0	0.0	0.0	0.0	0.0	0.0	0.0	0.0	0.0	0.0
9	RF	0.0	0.0	0.0	0.0	0.0	0.0	0.0	0.0	0.0	0.0	0.0
10	LUL	0.0	0.0	0.0	0.0	0.0	0.0	0.0	0.0	0.0	0.0	0.0
11	LLL	0.0	0.0	0.0	0.0	0.0	0.0	0.0	0.0	0.0	0.0	0.0
12	LF	0.0	0.0	0.0	0.0	0.0	0.0	0.0	0.0	0.0	0.0	0.0
13	RUA	0.0	0.0	0.0	0.0	0.0	0.0	0.0	0.0	0.0	0.0	0.0
14	RLA	0.0	0.0	0.0	0.0	0.0	0.0	0.0	0.0	0.0	0.0	0.0
15	LUA	0.0	0.0	0.0	0.0	0.0	0.0	0.0	0.0	0.0	0.0	0.0
16	LIA	0.0	0.0	0.0	0.0	0.0	0.0	0.0	0.0	0.0	0.0	0.0
17	RHA	0.0	0.0	0.0	0.0	0.0	0.0	0.0	0.0	0.0	0.0	0.0
18	LHA	0.0	0.0	0.0	0.0	0.0	0.0	0.0	0.0	0.0	0.0	0.0

TABLE 7. Output of Baseline Input Data Set. Pedestrian Impact. (Page 4 of 10)

VEHICLE DECELERATION INPUTS

VEHICLE AT REST -- PANELS MOVING AT 10 MPH

CARD# C

YAW	PITCH	ROLL	XIPS	(YIPS)	VTIME	ZIPS	XG(X)	XO(Y)	XO(Z)	NATAB	ATO	ADT
0.0	0.0	0.0	0.0	0.0	0.0	0.0	0.0	0.0	0.0	-2	0.0	0.500000

ROTATING VEHICLE LINEAR TIME HISTORY

PAGE NO. 1

TIME (SEC.)	LINEAR DECELERATIONS (G'S)			LINEAR VELOCITIES (IN./SEC.)			LINEAR DISPLACEMENTS (IN.)		
	X	Y	Z	X	Y	Z	X	Y	Z
0.0	0.0	0.0	0.0	0.0	0.0	0.0	0.0	0.0	0.0
0.50000	0.0	0.0	0.0	0.0	0.0	0.0	0.0	0.0	0.0

ROTATING VEHICLE ANGULAR TIME HISTORY

PAGE NO. 1

TIME (SEC.)	ANGULAR ACCELERATIONS (DEG/SEC.**2)			ANGULAR VELOCITIES (DEG/SEC.)			ANGULAR DISPLACEMENTS (DEG)		
	X	Y	Z	X	Y	Z	YAW	PITCH	ROLL
0.0	0.0	0.0	0.0	0.0	0.0	0.0	0.0	0.0	0.0
0.50000	0.0	0.0	0.0	0.0	0.0	0.0	0.0	0.0	0.0

TABLE 7. Output of Baseline Input Data Set. Pedestrian Impact. (Page 5 of 10)

PLANE INPUTS

PLANE NO.	1, NUMTIM=	2, NMATRL=	1, LEDGSW=	3, NINTRL=	0, ISOLAT=	0, WITH NAME OF	ROOF
TIMEFF	X1	Y1	Z1	X2	Y2	Z2	X3
0.0	71.6700	0.0	-49.8300	74.9000	36.0000	-49.8300	100.0000
1.0000	-104.3300	0.0	-49.8300	-101.1000	36.0000	-49.8300	-76.0000
Y3							Z3
							-49.8300
							-49.8300
PLANE NO.	2, NUMTIM=	2, NMATRL=	1, LEDGSW=	3, NINTRL=	0, ISOLAT=	0, WITH NAME OF	WINDSHIELD
TIMEFF	X1	Y1	Z1	X2	Y2	Z2	X3
0.0	51.0300	0.0	-37.1700	55.8400	36.0000	-37.1700	71.6700
1.0000	-124.9700	0.0	-37.1700	-120.1600	36.0000	-37.1700	-104.3300
Y3							Z3
							-49.8300
							-49.8300
PLANE NO.	3, NUMTIM=	2, NMATRL=	1, LEDGSW=	3, NINTRL=	0, ISOLAT=	0, WITH NAME OF	HOOD
TIMEFF	X1	Y1	Z1	X2	Y2	Z2	X3
0.0	6.5700	0.0	-31.7400	9.3400	36.0000	-31.7400	51.0300
1.0000	-169.4300	0.0	-31.7400	-166.6600	36.0000	-31.7400	-124.9700
Y3							Z3
							-37.1700
							-37.1700
PLANE NO.	4, NUMTIM=	2, NMATRL=	1, LEDGSW=	3, NINTRL=	0, ISOLAT=	0, WITH NAME OF	GRILL
TIMEFF	X1	Y1	Z1	X2	Y2	Z2	X3
0.0	3.5200	0.0	0.0	6.4500	36.0000	0.0	4.5100
1.0000	-172.4800	0.0	0.0	-169.5500	36.0000	0.0	-171.4900
Y3							Z3
							-29.5000
							-29.5000
PLANE NO.	5, NUMTIM=	2, NMATRL=	1, LEDGSW=	3, NINTRL=	0, ISOLAT=	0, WITH NAME OF	BUMPER
TIMEFF	X1	Y1	Z1	X2	Y2	Z2	X3
0.0	0.1700	0.0	0.0	2.1200	36.0000	0.0	0.0
1.0000	-175.8300	0.0	0.0	-173.8800	36.0000	0.0	-176.0000
Y3							Z3
							-26.0000
							-26.0000
PLANE NO.	6, NUMTIM=	1, NMATRL=	2, LEDGSW=	3, NINTRL=	0, ISOLAT=	0, WITH NAME OF	GROUND
TIMEFF	X1	Y1	Z1	X2	Y2	Z2	X3
0.0	-100.0000	100.0000	0.0	10.0000	100.0000	0.0	0.0
Y3							Z3
							-100.0000
							0.0
PLANE NO.	7, NUMTIM=	2, NMATRL=	3, LEDGSW=	3, NINTRL=	0, ISOLAT=	0, WITH NAME OF	GRILL TOP
TIMEFF	X1	Y1	Z1	X2	Y2	Z2	X3
0.0	4.5100	0.0	-29.5000	7.2900	36.0000	-29.5000	6.5700
1.0000	-171.4900	0.0	-29.5000	-168.7100	36.0000	-29.5000	-169.4300
Y3							Z3
							-31.7400
							-31.7400

TABLE 7. Output of Baseline Input Data Set. Pedestrian Impact. (Page 6 of 10)

ADDITIONAL ELLIPSOID INPUT

CARDS D-5

NO.	SEMIAXES (IN.)			OFFSET (IN.)			ROTATION (DEG)			ROLL
	X	Y	Z	X	Y	Z	YAW	PITCH		
1	0	0	0	0.0	0.0	0.0	0.0	0.0	0.0	0.0
2	0	0	0	0.0	0.0	0.0	0.0	0.0	0.0	0.0
3	0	0	0	0.0	0.0	0.0	0.0	0.0	0.0	0.0
4	0	0	0	0.0	0.0	0.0	0.0	0.0	0.0	0.0
5	0	0	0	0.0	0.0	0.0	0.0	0.0	0.0	0.0
6	0	0	0	0.0	0.0	0.0	0.0	0.0	0.0	0.0
7	0	0	0	0.0	0.0	0.0	0.0	0.0	0.0	0.0
8	0	0	0	0.0	0.0	0.0	0.0	0.0	0.0	0.0
9	0	0	0	0.0	0.0	0.0	0.0	0.0	0.0	0.0
10	0	0	0	0.0	0.0	0.0	0.0	0.0	0.0	0.0
11	0	0	0	0.0	0.0	0.0	0.0	0.0	0.0	0.0
12	0	0	0	0.0	0.0	0.0	0.0	0.0	0.0	0.0
13	0	0	0	0.0	0.0	0.0	0.0	0.0	0.0	0.0
14	0	0	0	0.0	0.0	0.0	0.0	0.0	0.0	0.0
15	0	0	0	0.0	0.0	0.0	0.0	0.0	0.0	0.0
16	0	0	0	0.0	0.0	0.0	0.0	0.0	0.0	0.0
17	0	0	0	0.0	0.0	0.0	0.0	0.0	0.0	0.0
18	0	0	0	0.0	0.0	0.0	0.0	0.0	0.0	0.0

BODY SEGMENT SYMMETRY INPUT

CARD D-7

SEG NO.	1	2	3	4	5	6	7	8	9	10	11	12	13	14	15	16	17	18
MSY(IJ)	0	0	0	0	0	0	0	0	0	0	0	0	0	0	0	0	0	0

MATERIAL NORMAL FORCE SPECIFICATION

CARD D-9-A

NMATRL	NAME	NSTM	NGRTAB	IFRIK	DC	DE	DF	FSAI	DM
1	PANEL MATERIAL	-1	-1	0	0.0	0.0	0.0	0.0	0.0
2	GROUND	-2	-1	1	0.0	0.0	0.0	0.0	0.0
3	GRILL TOP MAIL	-3	-1	0	0.0	0.0	0.0	0.0	0.0

TANGENTIAL FORCE SPECIFICATION

CARD D-9-B

FRIKC	MUO	MU1	MU2	A1	A2	FTMAX	VEL RAMP	LFNGTH.
1	0	0.1000000E+01	0.0	0.0	0.0	0.1000000E+04	0.1000000E+00	0.1000000E+00

BIVARIANT POLYNOMIAL SPECIFICATIONS

CARDS E-5-A-E-5-C

NPIDLY	1	0.10000000E+04	0.0	0.0	0.0	0.0	0.0	0.0
		0.0	0.0	0.0	0.0	0.0	0.0	0.0
		0.0	0.0	0.0	0.0	0.0	0.0	0.0
		0.0	0.0	0.0	0.0	0.0	0.0	0.0

TABLE 7. Output of Baseline Input Data Set. Pedestrian Impact. (Page 7 of 10)

2	0.47000000E+03	0.0	0.0	0.0	0.0	0.0	0.0
	0.0	0.0	0.0	0.0	0.0	0.0	0.0
	0.0	0.0	0.0	0.0	0.0	0.0	0.0
	0.0	0.0	0.0	0.0	0.0	0.0	0.0
	0.0	0.0	0.0	0.0	0.0	0.0	0.0
3	6.27000000E+04	0.0	0.0	0.0	0.0	0.0	0.0
	0.0	0.0	0.0	0.0	0.0	0.0	0.0
	0.0	0.0	0.0	0.0	0.0	0.0	0.0
	0.0	0.0	0.0	0.0	0.0	0.0	0.0
	0.0	0.0	0.0	0.0	0.0	0.0	0.0

TABLE 7. Output of Baseline Input Data Set. Pedestrian Impact. (Page 8 of 10)

ALLOWED CONTACTS AND ASSOCIATED FUNCTIONS

ELLIPSOID INDEX NAME	CONTACTS	PANEL INDEX NAME	OR	ELLIPSOID INDEX NAME
1	LOWER TORSO	2	WINDSHIELD	
1	LOWER TORSO	3	HOOD	
1	LOWER TORSO	7	GRILL TOP	
3	UPPER TORSO	1	ROOF	
3	UPPER TORSO	2	WINDSHIELD	
3	UPPER TORSO	3	HOOD	
5	HEAD	1	ROOF	
5	HEAD	2	WINDSHIELD	
5	HEAD	3	HOOD	
6	RIGHT UPPER LEG	3	HOOD	
6	RIGHT UPPER LEG	4	GRILL	
6	RIGHT UPPER LEG	7	GRILL TOP	
7	RIGHT UPPER LEG			10 LEFT UPPER LEG
7	RIGHT KNEE			
8	RIGHT SHIN	5	BUMPER	
9	RIGHT FOOT	5	BUMPER	
10	LEFT UPPER LEG	6	GROUND	
10	LEFT UPPER LEG	3	HOOD	
10	LEFT UPPER LEG	4	GRILL	
10	LEFT UPPER LEG	7	GRILL TOP	
11	LEFT LOWER LEG	5	BUMPER	
12	LEFT FOOT	6	GROUND	
13	RIGHT UPPER ARM	3	HOOD	
14	RIGHT LOWER ARM	3	HOOD	
15	LEFT UPPER ARM	3	HOOD	
16	LEFT LOWER ARM	3	HOOD	

SUBROUTINE INITIAL INPUT

ZPLT(X)	ZPLT(Y)	ZPLT(Z)	J1	J2	J3
10.00	30.00	1.00	0	0	0

INITIAL POSITIONS (INERTIAL REFERENCE)

SEGMENT NO. SEG	LINEAR POSITION (IN.)			LINEAR VELOCITY (IN./SEC.)		
	X	Y	Z	X	Y	Z
1	LT	-7.50000	15.00000	-33.72000	0.0	0.0
2	CT	-7.50000	13.80250	-30.57551	0.0	0.0
3	UT	-7.50000	11.44724	-47.36544	0.0	0.0
4	H	-7.50000	10.76366	-53.39393	0.0	0.0
5	H	-7.50000	8.53646	-57.45589	0.0	0.0
6	RUL	-4.70000	13.12931	-25.31889	0.0	0.0
7	URLL	-4.70000	10.84816	-17.12080	0.0	0.0
8	LRL	-4.70000	10.00305	-5.08009	0.0	0.0
9	RF	-4.70000	8.06086	-1.23980	0.0	0.0
10	LUL	-10.30000	16.65760	-25.07217	0.0	0.0
11	LLL	-10.30000	20.99785	-11.60614	0.0	0.0
12	LF	-10.30000	23.73856	-1.95785	0.0	0.0
13	RJA	0.19154	10.60399	-43.54496	0.0	0.0
14	RLA	0.49301	11.57020	-34.35210	0.0	0.0
15	LUA	-15.45880	10.59728	-43.60877	0.0	0.0
16	LLA	-15.83409	8.51251	-35.54758	0.0	0.0
17	RHA	-1.33864	12.16022	-28.73838	0.0	0.0
18	LHA	-13.79881	4.69622	-31.45510	0.0	0.0

INITIAL ANGULAR ROTATION AND VELOCITY

SEGMENT NO. SEG	ANGULAR ROTATION (DEG)			ANGULAR VELOCITY (DEG/SEC.)		
	YAW	PITCH	ROLL	X	Y	Z
1	LT	-90.00000	0.0	-15.00000	0.0	0.0
2	CT	-90.00000	0.0	-15.00000	0.0	0.0
3	UT	-90.00000	0.0	-15.00000	0.0	0.0
4	H	-90.00000	0.0	-15.00000	0.0	0.0
5	H	-90.00000	0.0	-15.00000	0.0	0.0
6	RUL	-90.00000	0.0	18.00000	0.0	0.0
7	URLL	-90.00000	0.0	6.00000	0.0	0.0
8	LRL	-90.00000	0.0	90.00000	0.0	0.0
9	RF	-90.00000	0.0	-10.00000	0.0	0.0
10	LUL	-90.00000	0.0	-25.00000	0.0	0.0
11	LLL	-90.00000	0.0	78.00000	0.0	0.0
12	LF	-90.00000	0.0	-6.00000	0.0	0.0
13	RUA	-90.00000	12.00000	-6.00000	0.0	0.0
14	RLA	-90.00000	-12.00000	-6.00000	0.0	0.0
15	LUA	-90.00000	-15.00000	-6.00000	0.0	0.0
16	LLA	-90.00000	15.00000	43.00000	0.0	0.0
17	RHA	-90.00000	-30.00000	-6.00000	0.0	0.0
18	LHA	-90.00000	30.00000	43.00000	0.0	0.0

LINEAR AND ANGULAR VELOCITIES HAVE BEEN SET EQUAL TO THE INITIAL VEHICLE VELOCITIES.

TABLE 7. Output of Baseline Input Data Set. Pedestrian Impact. (Page 10 of 10)

LINE	DATE	TIME	TYPE	DESCRIPTION	AMOUNT	DEBIT	CREDIT	BALANCE	ACCOUNT
1	17 APR 1980	000000000	1.	BASELINE PEDESTRIAN DATA SET					A-1-A
2									A-1-B
3									A-1-C
4									A-2
5									A-3
6									A-4
7									A-5
8									A-6-A
9									A-6-B
10									B-1
11									B-2
12									B-3
13									B-4
14									B-5
15									B-6
16									B-7
17									B-8
18									B-9
19									B-10
20									B-11
21									B-12
22									B-13
23									B-14
24									B-15
25									B-16
26									B-17
27									B-18
28									B-19
29									B-20
30									B-21
31									B-22
32									B-23
33									B-24
34									B-25
35									B-26
36									B-27
37									B-28
38									B-29
39									B-30
40									B-31
41									B-32
42									B-33
43									B-34
44									B-35
45									B-36
46									B-37
47									B-38
48									B-39
49									B-40
50									B-41
51									B-42
52									B-43
53									B-44
54									B-45
55									B-46

TABLE 8. Listing of Baseline Pedestrian Impact Input Data File. (Page 1 of 6)

176	12	0	LEFT FOOT	1.52	1.8	5.22	0.	0.	0.	0.	0.	0.5
177	13	13	RIGHT UPPER ARM	1.87	1.44	6.88	0.	0.	0.	0.	0.	0.5
178	14	14	RIGHT LOWER ARM	1.4	1.4	5.75	0.	0.	0.	0.	0.	0.5
179	15	15	LEFT UPPER ARM	2.07	1.64	6.88	0.	0.	0.	0.	0.	0.5
180	16	16	LEFT LOWER ARM	1.4	1.4	5.75	0.	0.	0.	0.	0.	0.5
181	17	17	RIGHT HAND	1.2	1.2	3.7	0.	0.	0.	0.	0.	0.5
182	18	18	LEFT HAND	1.2	1.2	3.7	0.	0.	0.	0.	0.	0.5
183	0	0	0	0	0	0	0	0	0	0	0	0.7
184	1	PANFL MATERIAL	-1	-1	0	0.	0.	0.	0.	0.	0.	0.9-A
185	2	GROUND	-2	-1	1	0.	0.	0.	0.	0.	0.	0.9-A
186	3	GRILL TOP MATL.	-3	-1	0	0.	0.	0.	0.	0.	0.	0.9-A
187	1	0	1.	0.	0.	0.	0.	1000.	0.	0.	0.	0.9-B
188	51											E.1
189	1	1000.										E.5-A
190	1											E.5-B
191	1											E.5-C
192	2	470.										E.5-A
193	2											E.5-B
194	2											E.5-C
195	3	2000.										E.5-A
196	3											E.5-B
197	3											E.5-C
198												E.5-A
199												E.5-D
200												F.1-A
201												F.1-B
202												F.1-B
203												F.1-B
204												F.1-A
205												F.1-A
206												F.1-B
207												F.1-B
208												F.1-B
209												F.1-A
210												F.1-A
211												F.1-B
212												F.1-B
213												F.1-B
214												F.1-A
215												F.1-B
216												F.1-B
217												F.1-B
218												F.1-B
219												F.1-A
220												F.1-B
221												F.1-A
222												F.1-B
223												F.1-A
224												F.1-B
225												F.1-B
226												F.1-A
227												F.1-B
228												F.1-B
229												F.1-A
230												F.1-B
231												F.1-A
232												F.1-B
233												F.1-A
234												F.1-B
235												F.1-A

TABLE 8. Listing of Baseline Pedestrian Impact Input Data File. (Page 4 of 6)

236													F-1-B
237	14	3											F-1-A
238	15	1											F-1-B
239	15	3											F-1-A
240	16	1											F-1-B
241	16	3											F-1-A
242	17	0											F-1-A
243	18	0											F-4-A
244	10.0				30.0			1.0					G-1
245	-7.5				15.			-33.72			0		1 G-2
246	-90.				0.0			-15.					1 G-3
247	-90.				0.0			-15.					2 G-3
248	-90.				0.0			-15.					3 G-3
249	-90.				0.0			-15.					4 G-3
250	-90.				0.0			-15.					5 G-3
251	-90.				0.0			18.					6 G-3
252	-90.				0.0			6.0					7 G-3
253	-90.				0.0			6.0					8 G-3
254	-90.				0.0			90.					9 G-3
255	-90.				0.0			-10.					10 G-3
256	-90.				0.0			-25.					11 G-3
257	-90.				0.0			78.					12 G-3
258	-90.				12.0			-6.					13 G-3
259	-90.				-12.			-6.					14 G-3
260	-90.				-15.			-6.					15 G-3
261	-90.				15.0			43.					16 G-3
262	-90.				-30.			-6.					17 G-3
263	-90.				30.			43.					18 G-3
264	16							0.0		0.0			H-1-A
265		1						0.0		0.0			2 H-1-B
266		3						0.0		0.0			3 H-1-B
267		5						0.0		0.0			4 H-1-B
268		6						0.0		0.0			5 H-1-B
269		7											6 H-1-B
270		8											7 H-1-B
271		9											8 H-1-B
272		10						0.0		0.0			9 H-1-B
273		11											10 H-1-B
274		12											11 H-1-B
275		13											12 H-1-B
276		14											13 H-1-B
277		15						0.0		0.0			14 H-1-B
278		16											15 H-1-B
279		17											16 H-1-B
280		18											H-2-A
281	0												H-3-A
282	16							0.0		0.0			2 H-3-B
283		1						0.0		0.0			3 H-3-B
284		3						0.0		0.0			4 H-3-B
285		5						0.0		0.0			5 H-3-B
286		6											6 H-3-B
287		7											7 H-3-B
288		8											8 H-3-B
289		9						0.0		0.0			9 H-3-B
290		10						0.0		0.0			10 H-3-B
291		11											11 H-3-B
292		12											12 H-3-B
293		13											13 H-3-B
294		14											14 H-3-B
295		15						0.0		0.0			15 H-3-B
		16											
		17											

TABLE 8. Listing of Baseline Pedestrian Impact Input Data File. (Page 5 of 6)

5.4 REPRESENTATIVE SIDE IMPACT OUTPUT

Figures 14 and 15 are a graphical presentation of some of the important kinematic variables produced by the computer exercise using the baseline side impact data. Figure 14 shows the major contact with the side structures at approximately 70 ms. By this time the space between the occupant and the side structures are used up. An additional major contact is noted at approximately 30 ms for the lower torso. This is caused by the intrusion of the lower door contact panel into the occupant compartment. This intrusion uses up the "slack" between the occupant and the side structures at an earlier point in time indicating the sensitivity of phasing of occupant contact with side structures to intrusion.

Figure 15 shows a trace of the motions of several body segments during the simulation. Lower torso excursion is relatively small due to the early interaction with side structures. The head pitches to the side but interacts only with the side header and B-pillar in this simulation. The fact that lower torso motion is limited prohibits the head from moving too far to the side.

Table 10 is a summary of all occupant/vehicle contact interactions. The time, deflection, and force are given for initiation of contact, peak force, and the final time of a contact event. In some cases it is seen that the peak force occurs at the end of the simulation. For a further study of the output, including cases of multiple peaks such as occurs for the lower torso, it is necessary to review the complete simulation output.

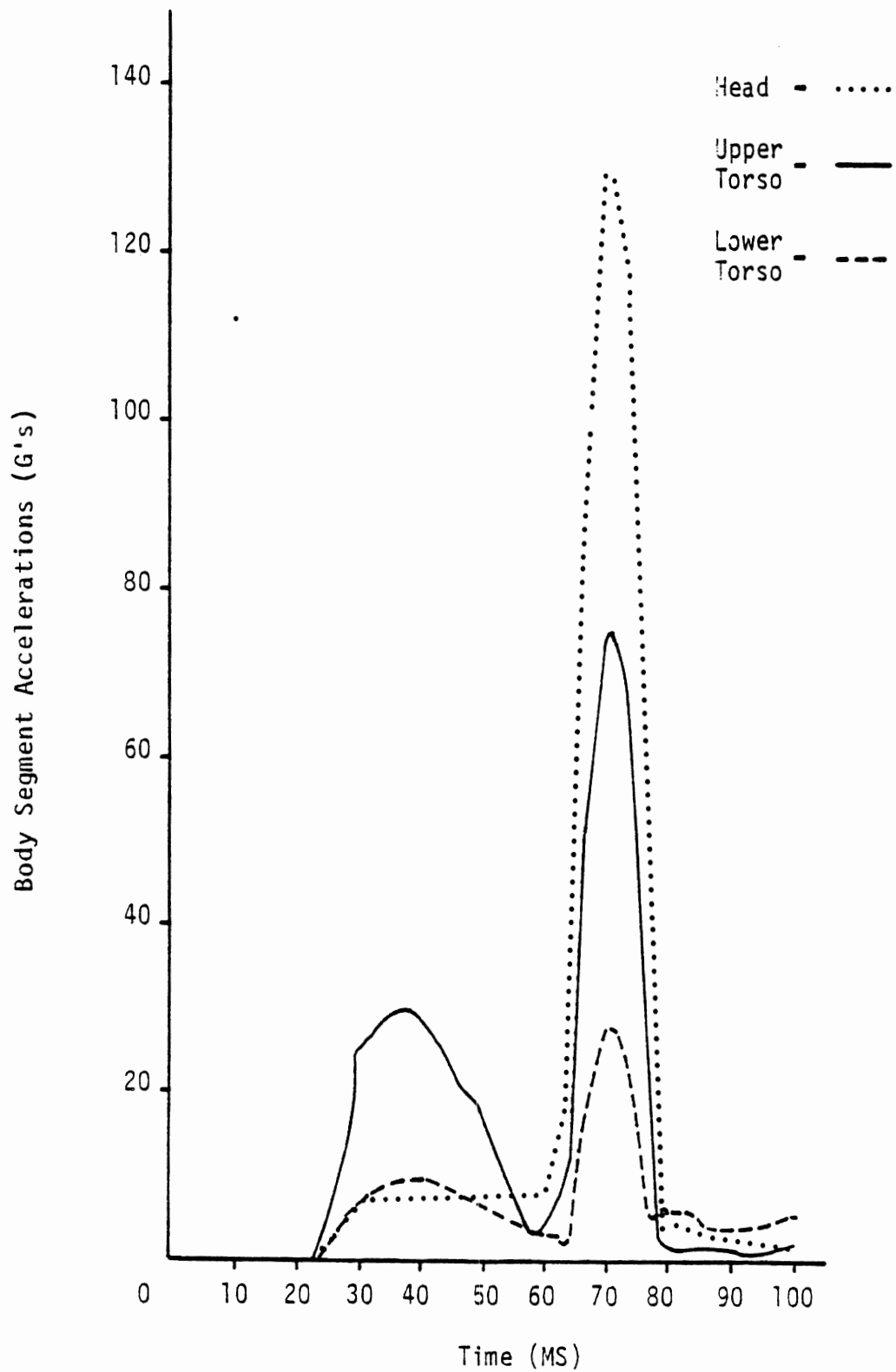


Fig. 14 Body Segment Accelerations. Side Impact

Dots are c-g positions every 5 ms. starting at 20 ms.

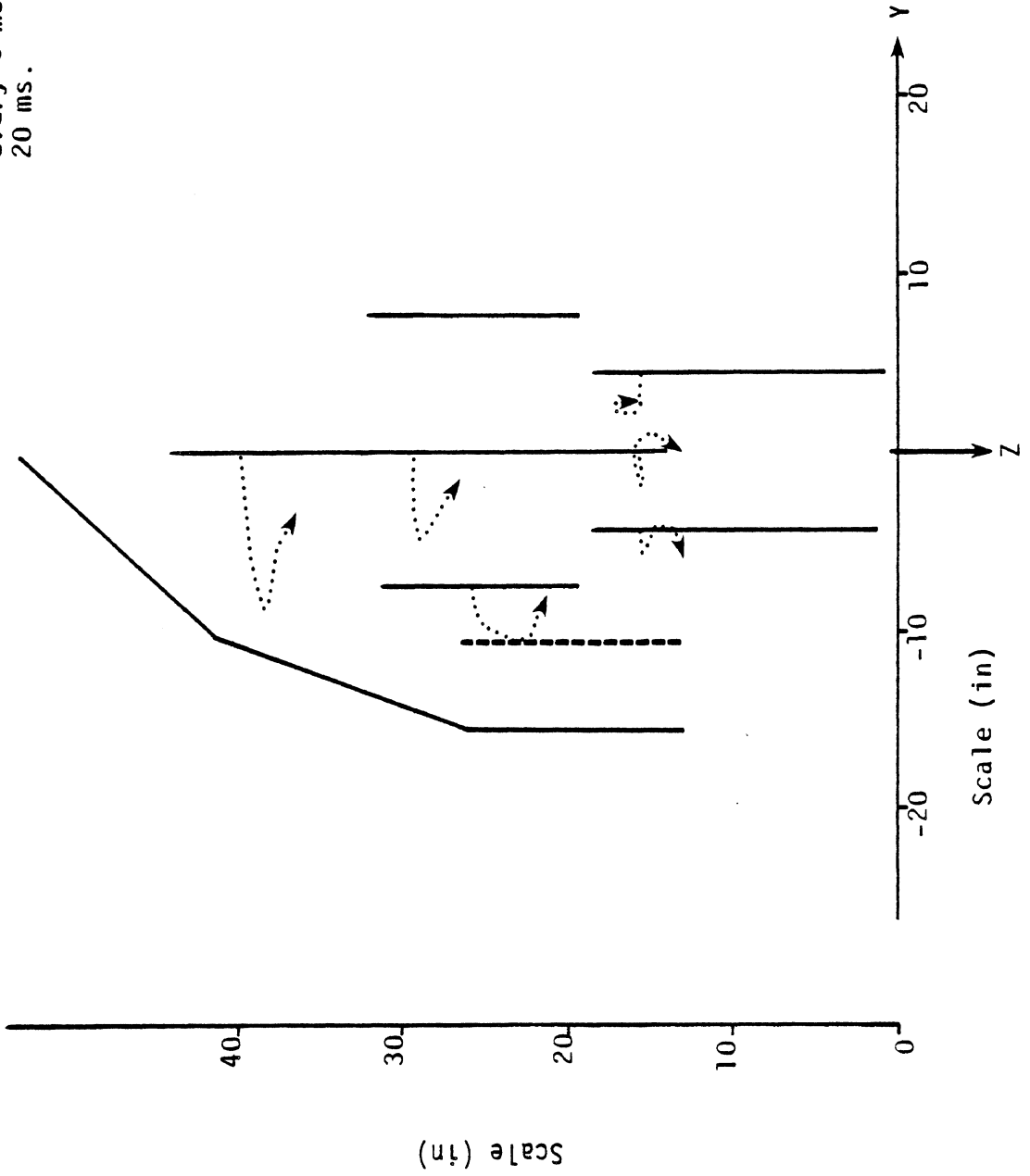


Fig. 15 Body Segment Motions. Side Impact.

TABLE 10. Side Impact Occupant Vehicle Contact History

Ellipsoid Name	Contact Name	Initial Contact			Peak Contact			Final Contact		
		Time (ms)	Deflection (in)	Force (1b)	Time (ms)	Deflection (in)	Force (1b)	Time (ms)	Deflection (in)	Force (1b)
LOWER TORSO	SEAT BACK	88	0.0	.3	100	0.1	4	100	0.1	4
LOWER TORSO	SEAT CUSHION	0	2.5	100	100	4.1	162	100	4.1	162
LOWER TORSO	HIP PANEL	28	0.1	93	39	0.9	929	57	0.0	12
UPPER TORSO	DOOR	60	0.1	66	71	0.9	668	81	0.0	14
HEAD	HEADER	62	0.1	119	70	1.0	965	78	0.2	149
HEAD	B-PILLAR	65	0.2	738	71	0.9	3579	78	0.1	274
RIGHT UPPER LEG	SEAT CUSHION	0	0.1	3	28	.1	4	36	0.0	1
		92	0.1	2	100	0.8	32	100	0.8	32
LEFT UPPER LEG	SEAT CUSHION	0	0.1	3	100	2.5	101	100	2.5	101
LEFT UPPER LEG	HIP PANEL	24	0.3	252	36	2.0	2002	100	0.7	675
LEFT FOOT	FLOOR	71	0.1	52	80	0.5	421	89	0.0	13
RIGHT UPPER LEG	LEFT UPPER LEG	50	0.0	40	60	0.8	783	100	0.0	47
RIGHT LOWER LEG	LEFT LOWER LEG	84	0.0	20	90	0.3	302	97	0.0	33

5.5 REPRESENTATIVE PEDESTRIAN IMPACT OUTPUT

Figure 16 includes a series of frames showing pedestrian kinematics at various time points during the exercise. The initial bumper contact with the lower right leg segments starts at 20 milliseconds and is over by 30 milliseconds. The grille, grille top and hood contact with the right upper leg and lower torso starts at 55 milliseconds and is over by 70 milliseconds. The pedestrian remains essentially upright throughout the time of initial contact involvement with the vehicle and for a long time thereafter.

Table 11 is a summary of all pedestrian/vehicle exterior contacts. As in Table 10, the time, deflection and force are given for initiation of contact, peak force and the final time of each contact event. Peak loads on the lower leg are somewhat in excess of human tolerance values for leg fracture. It is not known how the values compare with forces necessary to fracture the leg of a Part 572.

Figures 17-22 are plots of the G-levels predicted in several of the body segments. Generally the phasing of peak accelerations progresses from the initial leg contacts up through the head.

It should be noted that the torso segments, the head, and the neck operate as a single mass unit. The joints connecting these masses were locked with no unlocking torque provided. This contributes to the continuing upright position of the torso during much of the run. The addition of realistic flexibility to the spine would decrease this effect.

It should also be noted that the force-deflection curves used to govern the interactions between the vehicle and pedestrian are hypothetical and do not account for absorption of energy. This tends to increase the energy input to the lower extremities beyond what would normally be expected in a more realistic simulation.

In conclusion, the data set for simulation of a pedestrian interacting with the front of a vehicle is complete and functional. The location and shape of vehicle surfaces represents probably the most advanced information available. Likewise, position is based on human walking posture and a typical impact site both from the viewpoint of the vehicle

and the pedestrian. The leg fracture model is totally new. The two shortcomings in the data set relate to vehicle deformation properties and specification of joint properties in the pedestrian. Within the data framework already established it should not be difficult to improve these quantities when application to real vehicle problems is required.

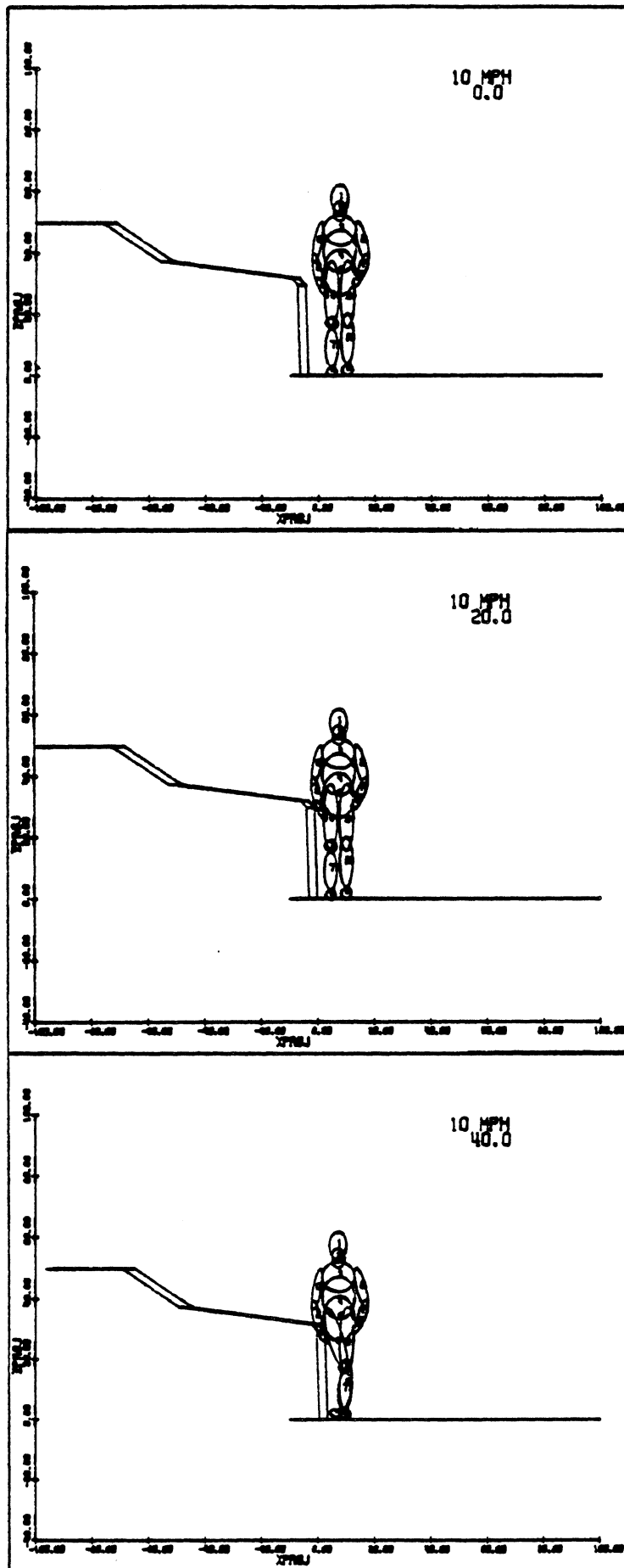


Fig. 16. Pedestrian Kinematics. (1 of 3; 0, 20, 40 ms)

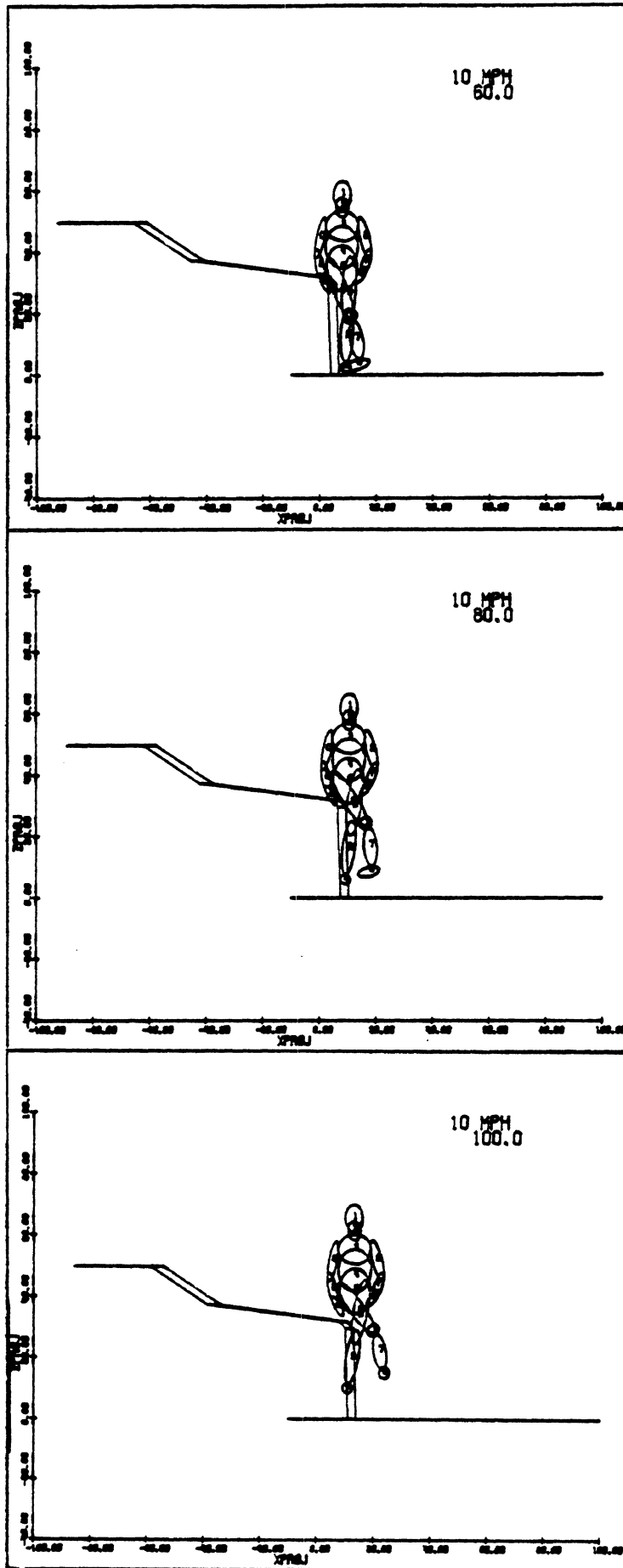


Fig. 16. Pedestrian Kinematics. (2 of 3; 60, 80, 100 ms)

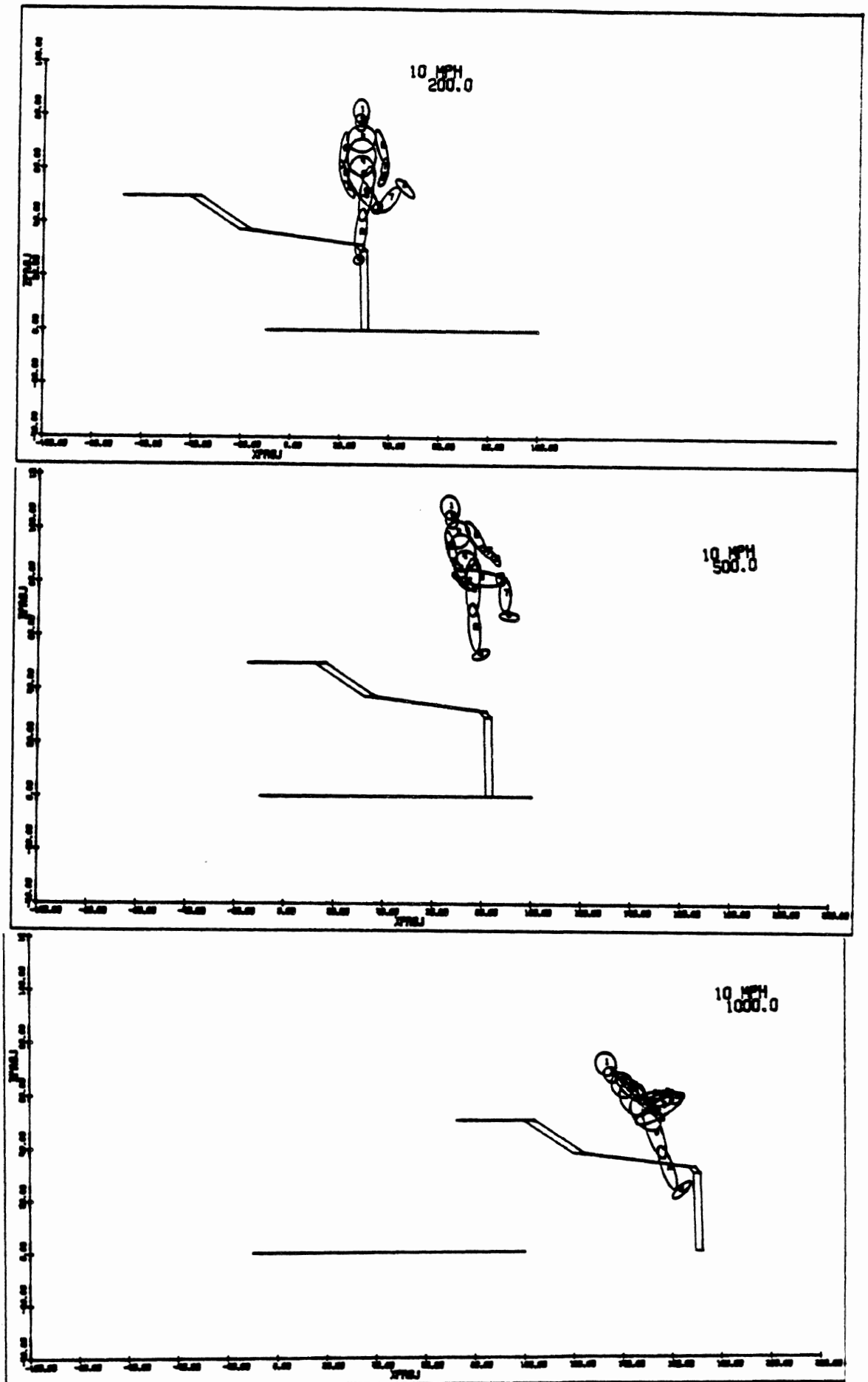


Fig. 16. Pedestrian Kinematics. (3 of 3; 200, 500, 1000 ms)

TABLE 11. PEDESTRIAN/VEHICLE CONTACT HISTORY

Ellipsoid Name	Contact Name	Initial Contact		Peak Contact		Final Contact				
		Time (ms)	Deflection (in)	Force (lb)	Time (ms)	Deflection (in)	Force (lb)	Time (ms)	Deflection (in)	Force (lb)
Lower Torso	Hood	65.	.03	35.	65.	.03	35.	65.	.03	35.
	Grille Top	55.	.31	611.	60.	.56	1127.	70.	.00	10.
Right Upper Leg	Grille Top	55.	.19	381.	65.	.85	1705.	70.	.28	567.
	Grille	55.	.12	122.	65.	.79	786.	70.	.24	244.
Right Knee	Bumper	20.	.45	454.	25.	.77	738.	30.	.07	70.
		60.	.73	732.	65.	.92	922.	70.	.05	53.
Right Shin	Bumper	20.	.41	410.	25.	.90	896.	30.	.47	474.
Right Foot	Ground	0.	.28	132.	0.	.28	132.	30.	.03	13.
Left Foot	Ground	0.	.08	38.	40.	.17	80.	45.	.11	53.
Right Lower Arm	Hood	40.	1.35	1352.	50.	3.01	3011.	70.	.52	518.
Right Upper Leg	Left Upper Leg	35.	.14	69.	80.	1.35	600.	295.	.00	2.

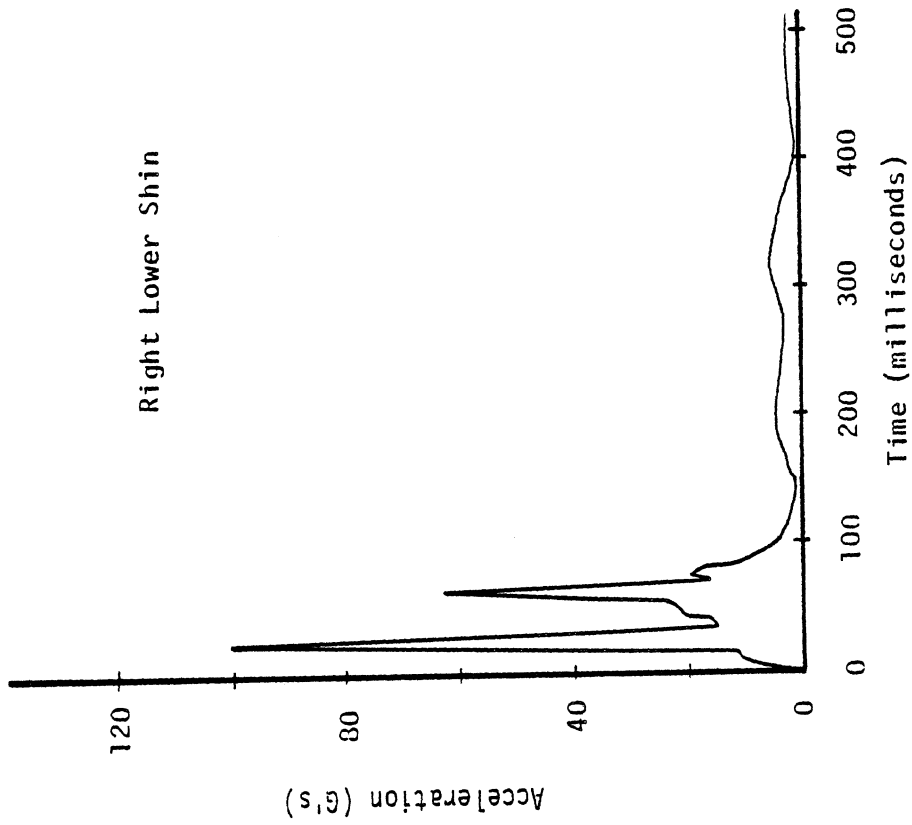


Fig. 18. Right Lower Shin Acceleration.
Pedestrian Impact (10 mph)

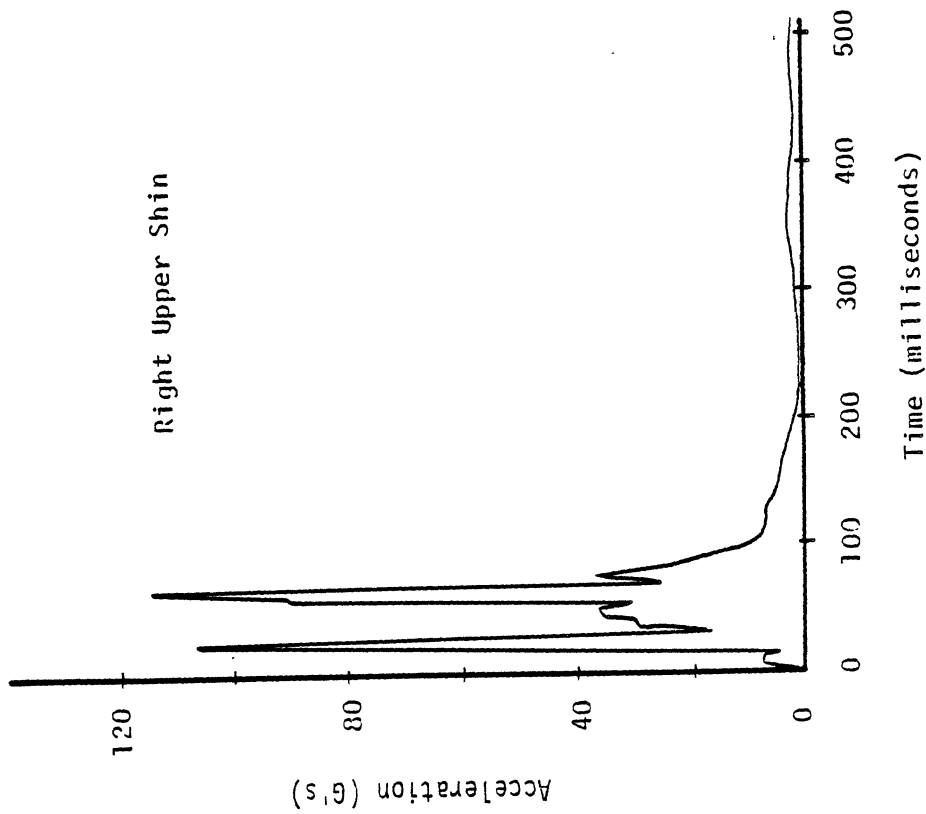


Fig. 17. Right Upper Shin Acceleration
Pedestrian Impact (10 mph)

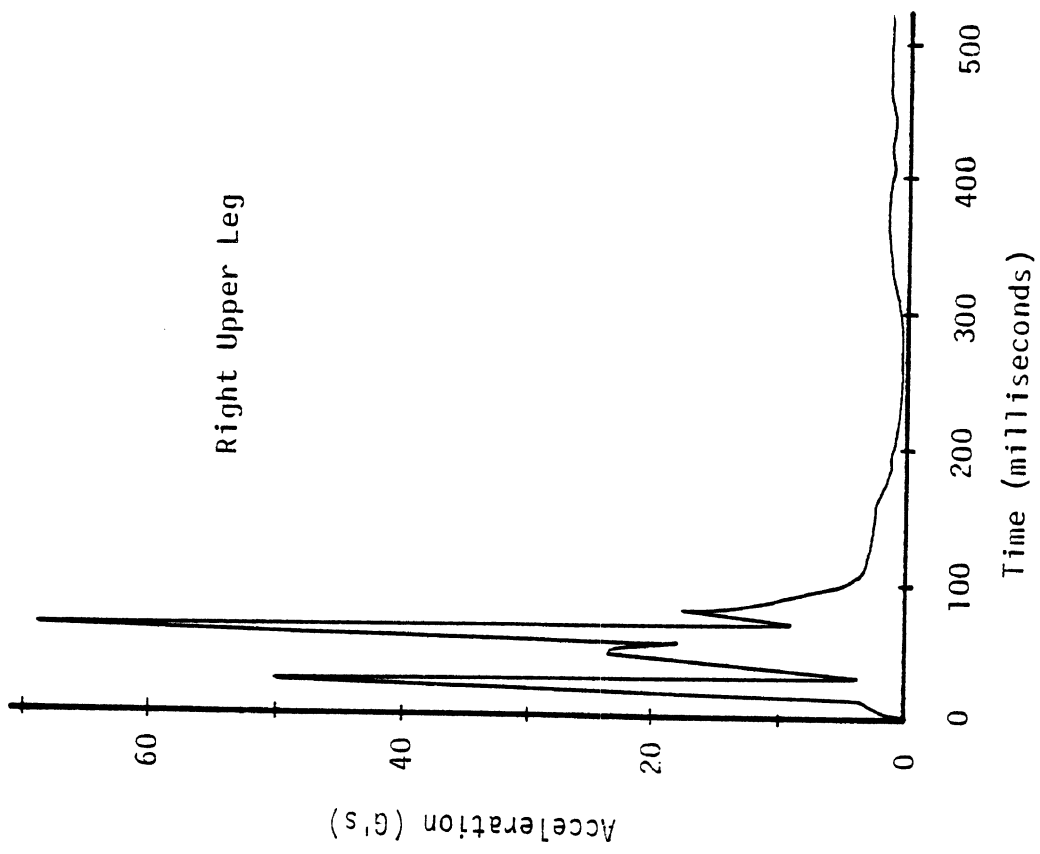


Fig. 19. Right Upper Leg Acceleration.
Pedestrian Impact (10 mph)

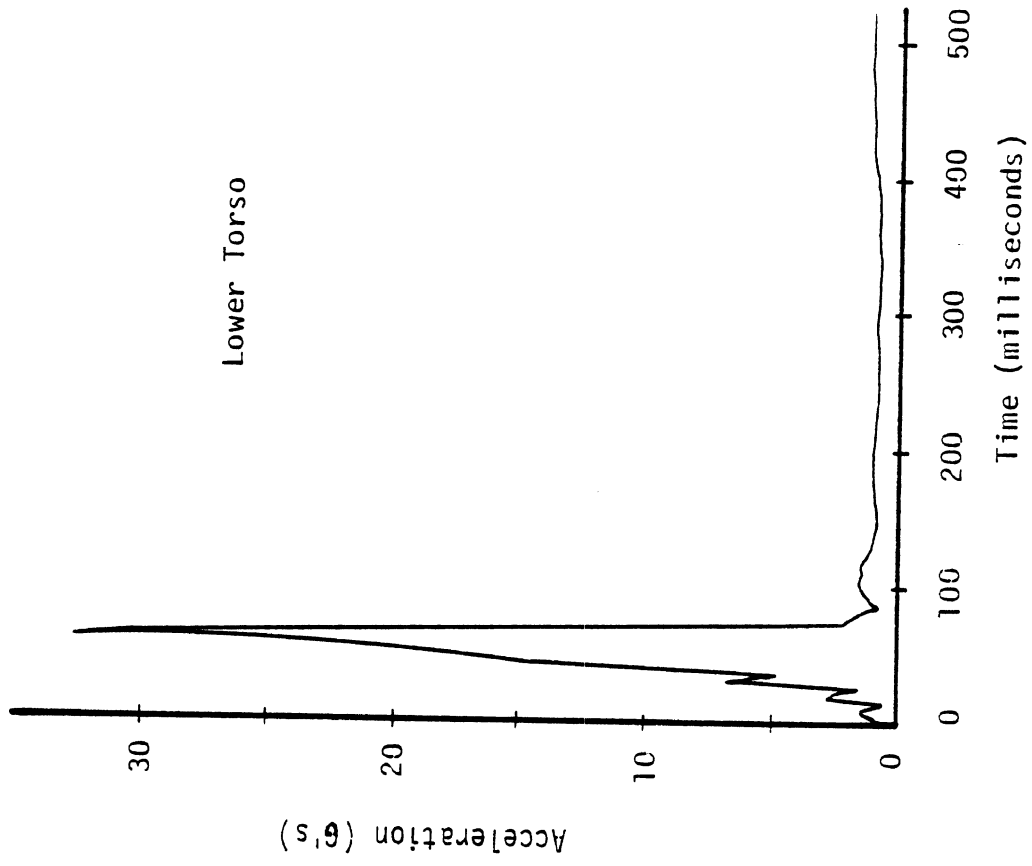


Fig. 20. Lower Torso Acceleration.
Pedestrian Impact (10 mph)

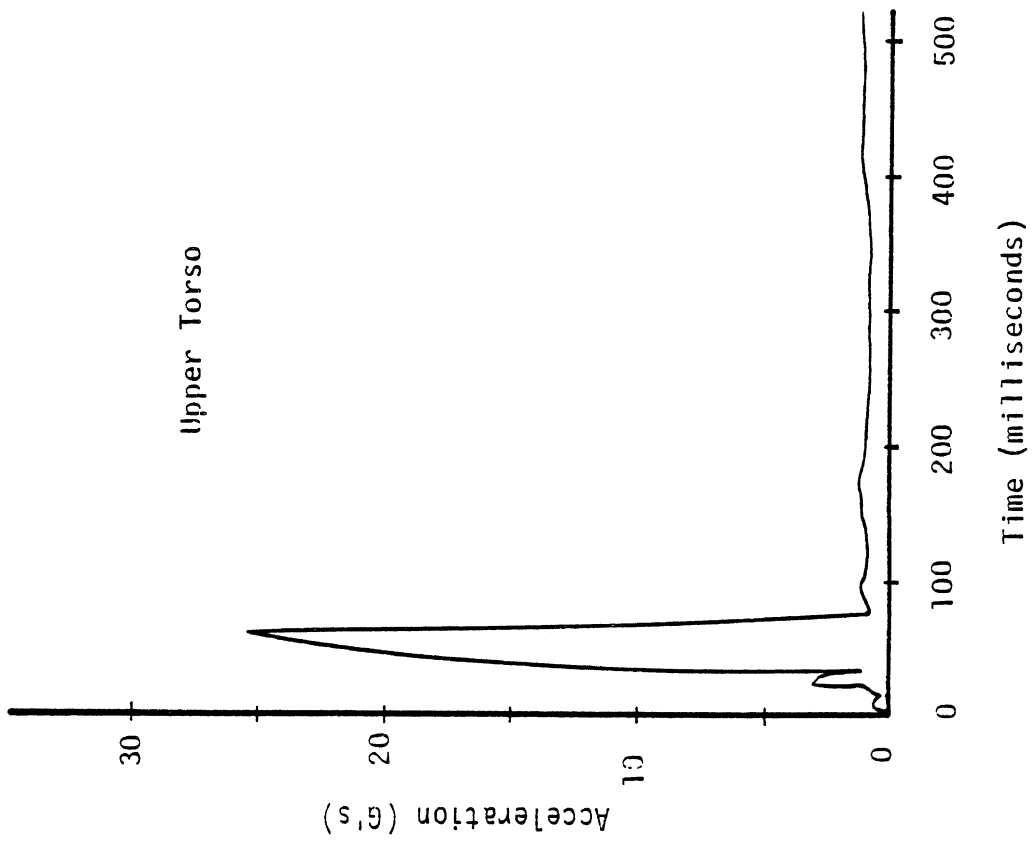


Fig. 21. Upper Torso Accelerations.
Pedestrian Impact (10 mph)

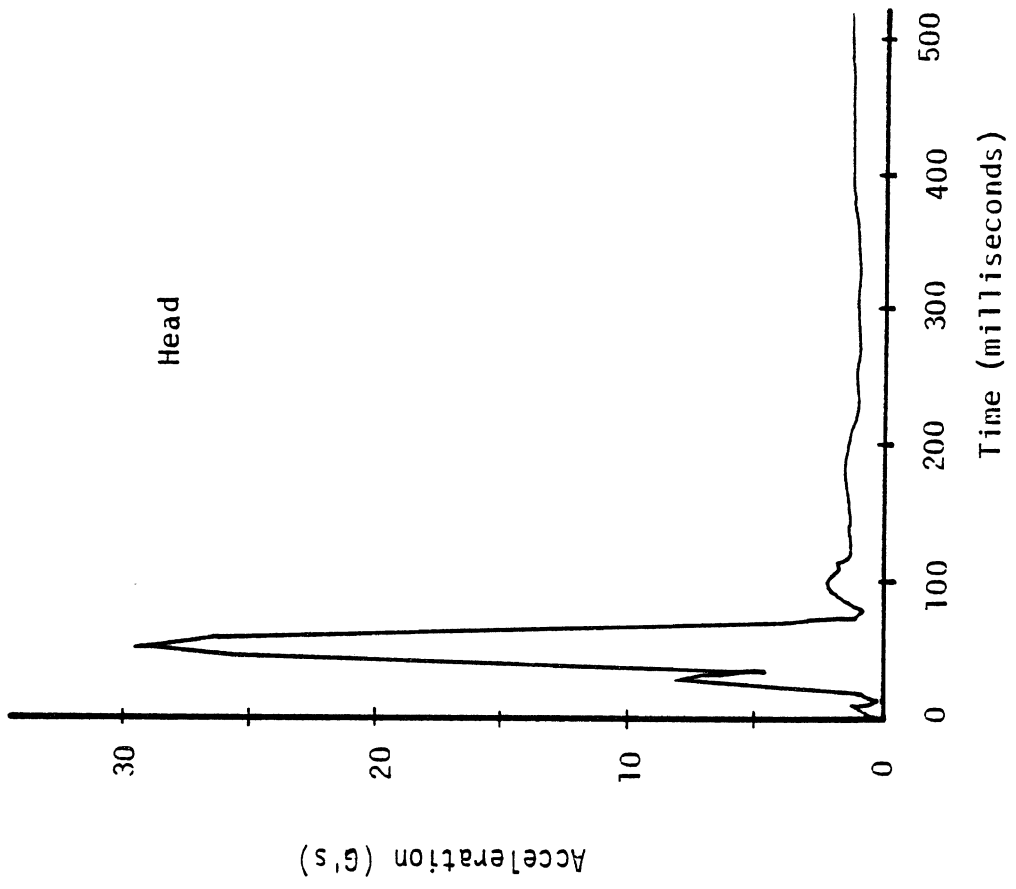


Fig. 22. Head Accelerations.
Pedestrian Impact (10 mph)

6.0 THE HSRI VERSION OF THE CALSPAN CVS

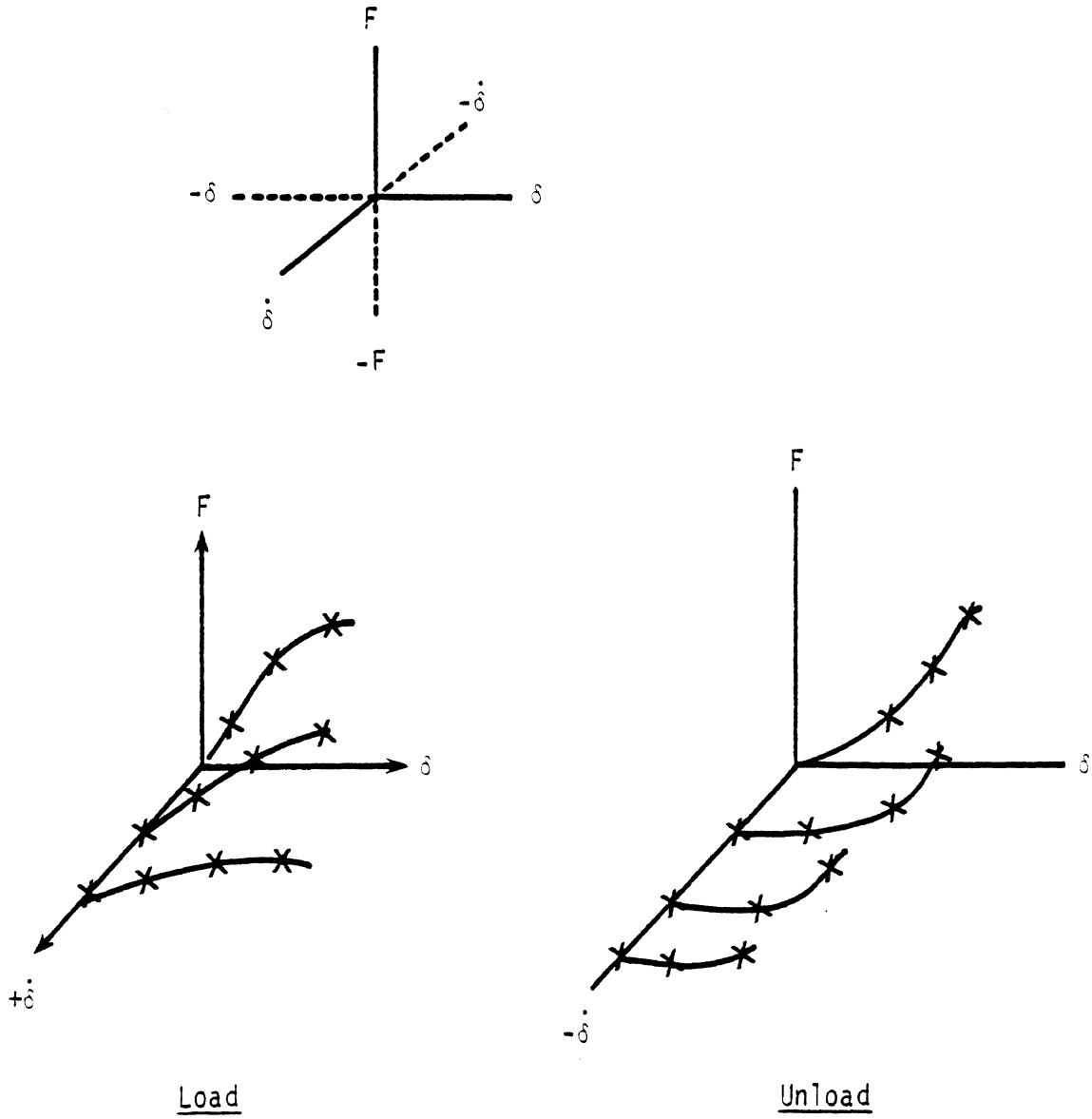
The HSRI version of the Calspan CVS has been and is being developed under NHTSA Contract No. DOT-HS-7-01659, "Occupant Side Impact Simulations Using CVS Program." The two sections of Part 6 describe the changes which have been made and the status of the code.

6.1 MODIFICATIONS TO ORIGINAL CALSPAN CVS PROGRAM

Several major and minor changes have been made to the original Calspan CVS program, Version 18-A, with some corrections being added from later Calspan issues. The most important changes have to do with the addition of mutual force-deformation properties for two contacting elements (ellipsoid/panel or ellipsoid/ellipsoid) and dynamic force-deflection relations. The concept of mutual deformation of contacting elements is drawn from earlier two- and three-dimensional modeling efforts at HSRI such as the MVMA 2-D model.

Figure 23 illustrates the means which has been coded for handling multiple dynamic force-deflection curves in the new CVS. It is first presumed that the rate of force application and deformation during a dynamic event (or computer simulation) is unknown ahead of time. In order to cope with this problem, it is necessary to have a description of material response under a range of dynamic loading conditions included as data with the operating program. A series of curves for different specimen loading and unloading rates may be available from an experimental program. Bivariate loading and unloading tables are the mechanism used to accomplish this. For the case of loading (+ δ) a series of curves are input at various loading rates. A similar series is shown for material unloading (- δ). The software interpolates through this load-unload space to select that force-deformation curve which actually occurs based on the space of known material response data. Crosses on the curves hint at our recommendation for manual intervention or simplification of experimental curves. The software has been tested and is functioning properly for trial cases. It remains to validate it with real experimental data.

Bivariate Force-Deflection - Deflection Rate Input



Input data from structural material tests.

Figure 23.

Force discontinuities at the edge of contact surfaces received considerable attention in order to include features of the MVMA 2-D software such as a transition zone as an ellipsoid slides off the edge and a penetration limit to avoid large forces when an ellipsoid starts out behind a contact surface. Figure 24 illustrates the means by which corner intersections of surfaces are handled in the new simulation. In the Calspan CVS all contact surfaces were independent of one another. As a result it was very easy for an ellipsoid to go "behind" a surface. This is particularly true for the case of pedestrian impact. British Leyland modified the CVS to avoid this problem and generated forces as shown in the upper of the two sketches. The MVMA 2-D model had a further capability of adjusting the force direction for a corner impact. Aspects of the British Leyland and HSRI concepts were combined for a new 3-D corner simulation for use with the HSRI version of the CVS.

Several additional changes should also be mentioned. As has been described earlier in this report, moving contact surfaces with respect to a vehicle (or inertial) coordinate system have been added to facilitate the study of intrusion. Code corrections have been made to the ellipsoid versus ellipsoid contact interaction so that one may not "pass through" the other. To facilitate studies of side, oblique, and general six-dimensional deceleration events the software was modified to ease the burden of the user in setting up vehicle geometry in strange coordinate systems. Finally more output categories were provided for useful physical quantities and for kinematics in inertial coordinates.

Table 12 briefly summarizes the quantity of code which is new to the HSRI version of the Calspan CVS. There are 24 new routines. Most of these deal with the contact between surfaces and ellipsoids, the generation of mutual deformation of surfaces, and the inclusion of dynamic deflection rate terms. Major changes refer to changes of approximately two-thirds of the code while minor changes involve one-third. "No" changes indicates that the only changes were in dimension size and array names. It is estimated that approximately one third of the code is new.

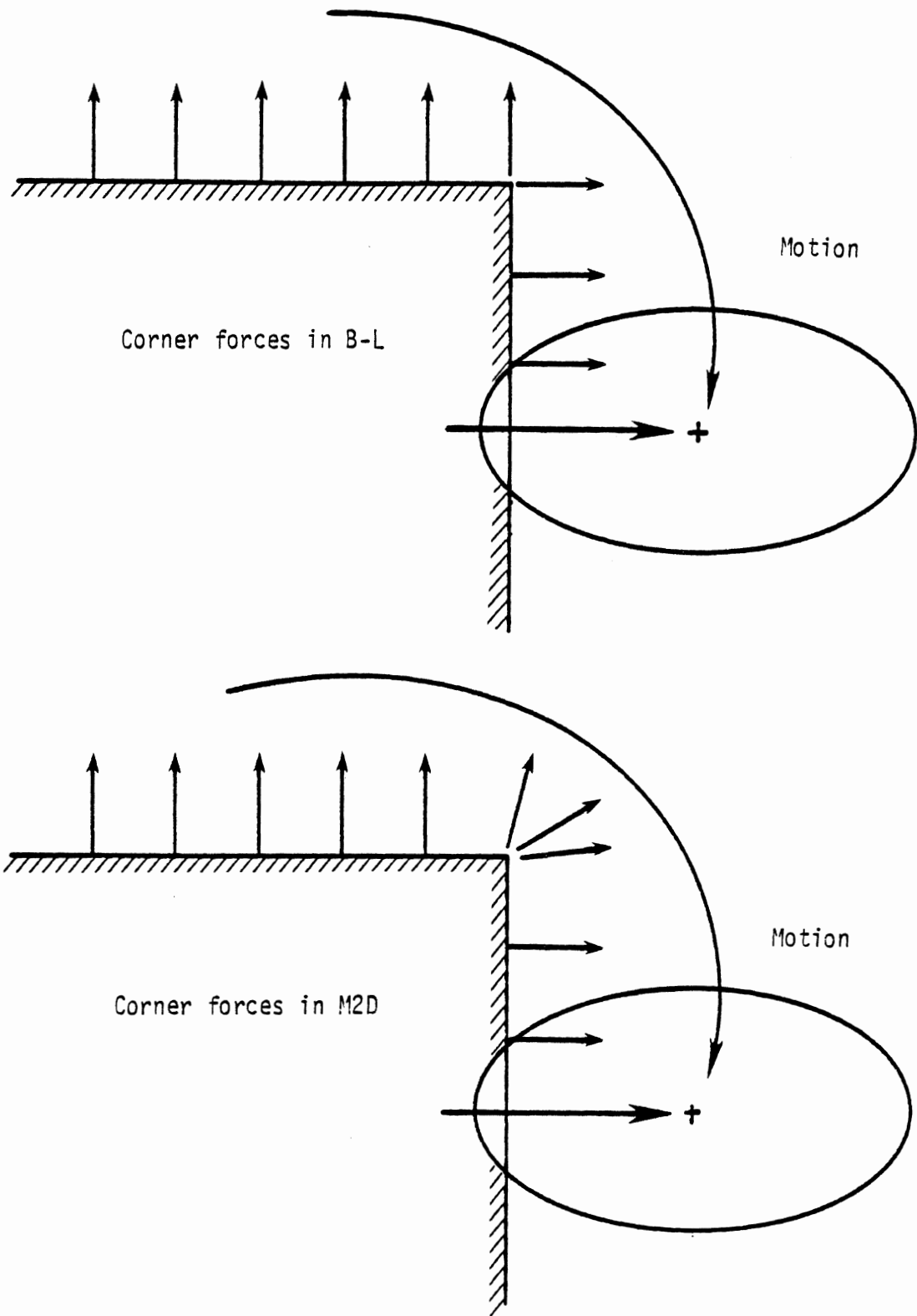


Fig. 24. Corner forces in British Leyland and MVMA 2-D Software

TABLE 12. CVS CODE CHANGES

- New routines	-	24
- Major changes	-	6
- Some changes	-	10
- "No" changes	-	72

6.2 STATUS OF SOFTWARE

The software which has been used in this project is functional and appears to operate correctly on the baseline data sets. Formal documentation of the algorithms will be initiated in early 1981. Only a summary input description for the various data cards has been delivered to the sponsor. The original contract on which this software was developed was scheduled for completion, including development of documentation and delivery of tapes, at the end of 1979. That schedule was in effect as we initiated this MVMA project. However, the sponsor requested modifications of HSRI work efforts in order to concentrate on development of a side impact dummy thorax. This has delayed completion of the documentation to the current estimate of mid-1981.

7.0 REFERENCES

1. Fleck, J. T., et al, "An Improved Three Dimensional Computer Simulation of Vehicle Crash Victims," 4 volume report on Contract No. DOT-HS-053-2-485, NTIS Nos. PB241692,3,4,5, April 1975.
2. Hubbard, R. P. and McLeod, D. G., "Geometric, Inertial, and Joint Characteristics of Two Part 572 Dummies for Occupant Modeling," SAE Paper No. 770937, Proc. 21st Stapp Car Crash Conf., pp. 933-972, October 1977.
3. Karnes, R. N., "CAL3D Crash Victim Simulation Computer Program User Manual," Report on MVMA Contract No. BCS 7501-C4.16, Boeing Computer Services, March 1975.
4. Viano, D. C. and Culver, C. C., "Performance of a Shoulder Belt and Knee Restraint in Barrier Crash Simulations," SAE Paper No. 791006, Proc. 23rd Stapp Car Crash Conf., pp. 105-132, October 1979.
5. Kramer, M., "Pedestrian Vehicle Accident Simulation Through Dummy Tests," SAE Paper No. 751165, Proc. 19th Stapp Car Crash Conf., pp. 705-724, November 1975.
6. Padgaonkar, A. J. and Prasad, P., "Simulation of Side Impact Using the CAL3D Occupant Simulation Model," SAE Paper No. 791007, Proc. 23rd Stapp Car Crash Conf., pp. 133-158, November 1979.
7. Siemonsen, H. D. and Bruckner, F., "Impacts on Plates, Particularly Glass Plates," SAE Paper No. 670924, Proc. 11th Stapp Car Crash Conf., pp. 293-298, November 1967.
8. Twigg, D. W. and Tocher, J. L., "Pedestrian Model Parametric Studies," 2 vol. report under Contract No. DOT-HS-356-3-719, NTIS Nos. DOT-HS-802419, 20, June 1977.